scientific reports

Check for updates

OPEN

Influence of ceramic thermal barrier coating on diesel engine performance using scum oil biodiesel at different compression ratios

Krishnamurthy K. N.[1]✉, B. N. Akash Deep[2], Venkatesh Birur Jayanna[1], C. P. Sumalatha[3], Anwar Khan[4,9], Sarfaraz Kamangar[5], Saiful Islam[6], Abdul Razak[7] & Yohanis Dabesa Jelila[8]✉

The present work explores the synergistic impact of mullite-based thermal barrier coatings (TBCs) and varying compression ratios (CRs) on the performance, combustion, and emission behavior of a single-cylinder, four-stroke variable compression ratio (VCR) diesel engine operated with Scum Oil Methyl Ester (SOME) diesel fuel blends. Mullite ceramic ($3Al_2O_3{\cdot}2SiO_2$) was applied via plasma spraying onto engine components including the piston crown, cylinder head, and intake/exhaust valves to minimize thermal losses. Experimental tests were carried out at CRs of 16.0, 17.5, and 19.0 using conventional diesel and blends of SOME (B20, B40, B60, B80, and B100 samples) in both coated and uncoated engine setups. The coated engine exhibited its best performance at CR 19, recording a BTE improvement of 7.51% for diesel and 5.75% for B20, alongside BSFC reductions of 14.28% and 9.09%, respectively, compared to the uncoated configuration. Additional enhancements were observed in terms of peak in-cylinder pressure, heat release rate, combustion efficiency, and reduced ignition delay and combustion duration. Emission measurements showed notable decreases in CO, HC, and smoke11.41%, 10.56%, and 9.43% for B20, and 6.16%, 7.10%, and 8.84% for diesel while only slight increases in NO_x and CO_2 emissions were recorded. These findings highlight the effectiveness of combining biodiesel and thermal barrier coatings in achieving improved efficiency and lower emissions, with the B20 blend at CR 19 showing the most favorable results for sustainable diesel engine operation.

Keywords Scum oil, Mullite coating, Low heat rejection engine, Variable compression ratio, Diesel engine performance, Combustion characteristics, And emission analysis

Energy demand worldwide is increasing drastically because of robust industrialization, transportation, rising population, rapid augmentation in shipping activities and expanding urbanization[1]. The increasing fuel price and extensive consumption of fossil fuels, derived from various fuel reserves like crude oil, coal, and conventional natural gas, is required to supply the world's energy needs[2]. Global warming threatens the environment due to the rapid increase in fuel burning. Since fossil fuels are depleting, many scientists are considering renewable, economically viable alternative fuels. In the past few decades, biodiesel production and consumption have

[1]Department of Mechanical Engineering, Centre for Post Graduate Studies, Visvesvaraya Technological University, Mysuru, Karnataka 570029, India. [2]Department of Mechanical Engineering, K.S. School of Engineering & Management, Bengaluru 560109, Karnataka, India. [3]Department of Mechanical Engineering, Government Polytechnic, Mandya District, Arakere, Srirangapatna 571415, Karnataka, India. [4]Department of Mechanical Engineering, Graphic Era (Deemed to be University), Dehradun 248002, Uttarakhand, India. [5]Mechanical Engineering Department, College of Engineering, King Khalid University, Abha 61421, Saudi Arabia. [6]College of Engineering, King Khalid University, Abha 61421, Saudi Arabia. [7]Department of Mechanical Engineering, P. A. College of Engineering (Affiliated to VTU), Mangaluru 574153, Karnataka, India. [8]Faculty of Mechanical Engineering, Jimma Institute of Technology, Jimma University, P.O. Box. 378, Jimma, Ethiopia. [9]Centre for Research Impact & Outcome, Chitkara University Institute of Engineering and Technology, Chitkara University, Rajpura 140401, Punjab, India. ✉email: krishnamurthykn1931@gmail.com; yohanis.jelila@ju.edu.et

become the center of attraction because of its renewability, bio-degradable, non-noxious, sustainable and eco-friendly. To meet the growing energy demand, biofuel ranks first among all other alternative energy sources[3].

Biodiesel is contented to as green energy due to reduction in emission from transport industry, because it has less aromatic compound content, it is carbon neutral, free from sulphur content and has 10–12% excess oxygen by weight[4]. These attributes lead to decrease in pollution by reducing the greenhouse gas (GHG) effluents such as CO, CO_2, unburnt HC and soot emissions. Biodiesel is a clean energy that provides potential advantages to human health with a reduction in particulate matter released into the atmosphere[5]. It has been found that overall biodiesel production cost, about 75% cost, will be for feedstock alone, therefore selecting a suitable raw material place and important role to ensure lower production cost. Biodiesel made from inedible vegetable oil costs 1.5 times more than diesel[6]. This made many researchers search for better alternative fuel to produce biodiesel at competitive and lower cost than that of non-edible vegetable oil. In the present study, dairy wash water scum is utilized as a low-cost, renewable feedstock for biodiesel production. In a developing country like India, large-scale milk dairies produce approximately 250 million tons of milk annually, generating around 400–500 kg of scum per day as a semi-solid industrial waste. This scum comprising fats, waste butter, ghee residues, lipids, proteins, and other solids floats on the surface of liquid effluents due to its lower density. The disposal of such waste poses significant challenges, including space constraints, foul odour, and environmental pollution. Moreover, it places an additional burden on effluent treatment plants, both operationally and economically. These factors highlight the urgent need for sustainable waste management practices. Motivated by this, the current research explores the use of dairy scum oil for the synthesis of scum oil methyl ester (SOME) as a clean-burning, eco-friendly alternative fuel in variable compression ratio (VCR) diesel engines, thereby addressing both energy and environmental concerns[7]. Diesel engines are adopted widely for their high thermal efficiency and robustness in transportation, agriculture, and electricity sectors. But reliance on petroleum-based fuels leads to Green House Gases and air pollution - a significant challenge to climate change and public health[8]. Thus, ICEs are the main origins of environmental pollutants, including carbon monoxide (CO), hydrocarbons (HC), nitrogen oxides (NO_x) and particulate matter (PM)[9].

Scum oil, a semi-liquid waste by-product from dairy wastewater treatment, offers a promising low-cost feedstock for biodiesel production. Unlike seed-based oils that require energy-intensive extraction and yield only 30–40% oil by weight, scum oil can be directly utilized, reducing upstream processing costs. Its conversion into biodiesel not only adds value to a typically discarded waste but also supports sustainable fuel production. Economically, it offers significant potential to reduce reliance on imported diesel, lower production costs, and promote circular waste management practices. Environmentally, its use helps curb illegal disposal, pollution, and ecological degradation. Moreover, the favorable combustion properties of scum biodiesel makes it a viable alternative fuel for CI engines, aligning with national goals for cleaner energy and waste-to-energy integration[10]. Direct use of straight non-edible oil/scum oil as alternative fuel for compression ignition (CI) diesel engines without modification affects combustion performance and engine parts. The most serious problems caused in the direct use of scum oil is poor atomization, fuel filter clocking and injector sticking, which leads to incomplete combustion due to higher viscosity, free fatty acid content, and density, non-volatility, as well as oxidation causes gum formation and higher lubricating leads to oil thickening[11]. When scum oil is used directly, carbon buildup on the fuel injector, valve, and seat causes engine fouling and chokes the injector after a few hours. However, for two decades, numerous researchers have worked to convert raw vegetable oil into biodiesel, which performs similarly to diesel fuel in CI engines. The high viscosity of vegetable oil due to its huge molecular mass and chemical structure is converted into biodiesel for engine use by different techniques. Transesterification is the most important method for converting triglycerides (oil/fats) with alcohol (methanol/ethanol) and catalyst (homogeneous/heterogeneous) at a certain temperature and time to ester (methyl/ethyl) and glycerol[10]. Transesterification of scum oil produces biodiesel with a higher calorific value, cetane number, and viscosity than crude scum oil, resulting in longer combustion time, shorter ignition delay (ID), and lower particulate emissions. Even after undergoing transesterification, biodiesel fuels still exhibit certain limitations such as high viscosity, suboptimal atomization, and poorer heating value when compared to conventional diesel fuel. However, biodiesel shares similar fuel characteristics to diesel, but its increased thickness requires engine adjustments to ensure its efficient utilization in diesel engines. Although diesel engines can only use diesel fuel, several researchers have proposed ways to alter engine design parameters like CR, fuel injector parameter, combustion chamber geometry, and TBC for engine elements to improve engine performance, combustion, and emissions with biodiesel. According to research, ceramic thermal barrier coating on engine components improves reliability, durability, thermal efficiency, combustion temperature, and biodiesel emission[12,13].

In compression ignition (CI) engines, only about 30–40% of the fuel's energy is converted into useful brake power. The remainder is lost through exhaust gases (30–35%), coolant (20–25%), friction and mechanical losses (5–10%), and minor losses from unburnt fuel and radiation. These values vary with engine design, load, and fuel properties. In principle, CI engines can improve thermal efficiency by releasing less heat while conforming to the second rule of thermodynamics. Consequently, the basic concept of TBC is to develop the low heat rejection (LHR) engine which decreases heat loss to the coolant and utilizes the energy to convert into useful work[14]. Thermal barrier-coated (TBC) engines reduce heat loss from the combustion chamber by insulating key components, thereby increasing in-cylinder temperatures. This thermal retention leads to improved combustion efficiency and shorter ignition delay. While higher combustion temperatures are typically linked to steeper pressure rise, the altered combustion characteristics in TBC engines particularly the shift toward diffusion-controlled combustion result in a more gradual pressure build-up. This contributes to enhanced thermal efficiency, increased exhaust energy availability, improved fuel economy, and reduced emissions of HC, CO, and smoke, along with lower combustion-induced noise due to smoother pressure rise[15]. Some investigations have shown four combustion property differences between LHR diesel engines and conventional diesel engines and. (a) the time it takes for ignition is reduced; (b) the period of burning caused by fuel-air mixing is lengthened

while the period caused by pre-mixing is decreased; (c) the overall duration of combustion increases; and (d) the rate at which heat is released during burning is reduced[16].

In ceramic TBC engines, the combustion chamber temperature is approximately 200–250 °C higher than in uncoated diesel engines. This higher temperature allows for the use of a wider variety of fuels with a broad distillation range, including lower quality fuels. Reduced heat rejection to the coolant raises gas temperature in the combustion chamber after compression, making cold weather easier and minimizing uncontrolled combustion knocking and noise[17]. While the concept of LHR engines is promising, with some studies indicating reduced heat rejection to cooling water, enhanced thermal efficiency, and improved energy availability in the exhaust, other experimental research, as noted in references and, found no improvement in thermal efficiency[18]. Authors show that TBCs' thermo-physical qualities, such as porosity and surface roughness, affect unburnt HC due to surface quenching and residual HC retention in the pores. The bond coat oxidation and the mismatch in thermal expansion between the metallic bond coat and the top ceramic layer, are the two significant disadvantages of TBCs[19,20]. TBCs on diesel engine components protect against high-temperature oxidation, corrosive environments, and metal fatigue by maintaining lower temperatures and converting available heat into useful energy[21]. According to **Bose 2007**[22] TBCs are multi-layered and consist of multiple materials applied to engine surfaces to provide thermal protection from hot combustion gases, thereby reducing the surface temperature of substrate components. Typically, TBC systems comprise three layers over the metal surface substrate: (1) a metallic bond coat (BC), (2) an intermediate thermally grown oxide (TGO), and (3) a ceramic material topcoat (TC). The mechanical, thermal, and physical properties of these layers largely depend on processing conditions. Research has explored various TBC materials for diesel engine components, including silicon carbide, fly ash, TiO_2, Al_2O_3, mullite ($3Al_2O_3.2SiO_2$), CaO/MgO-ZrO_2, yttria-stabilized zirconia (YSZ), $La_2Zr_2O_7$, $LaPO_4$, $BaZrO_3$, CeO_2, and lanthanum aluminate ($LaMgAl_{11}O_{19}$)[23].

Currently the most popular TCB material was partially stabilized yttria –zirconia (8% Y_2O_3-ZrO_2). Due to more quantity of oxygen vacancies in YSZ material which assists oxygen saturation at a peak temperature, causes oxidation of bond coat layer leads to decline in ceramic coatings. To break the bottleneck, several authors have tried to synthesize a novel material for thermal barrier coating as an alternative to zirconia-based material. Among the mentioned ceramic materials, in the current research work mullite material (aluminosilicate-$3Al_2O_3.2SiO_2$) as TBC has a greater potential which replace YSZ. Because it has low coefficient of thermal expansion, high thermal conductivity, low oxygen permeability, good thermal and chemical stability, creep resistance in oxidative and corrosive environments, high resistance to crack propagation and high thermal shock resistance[24]. There are different techniques developed by many researchers for coating TBC on the surface of the substrate such as chemical vapour deposition, plasma spraying technique, physical vapour deposition and flame spraying technique. But many literatures studies state that plasma spraying method for deposition of mullite coating on engine components is more competitive due to less cost, high stability with deep penetration and higher deposition rate compared to other methods. With the use of controlled thickness of nanoparticle multilayer mullite coating is gaining importance in the recent studies of LHR diesel engine. Because it increases the lifespan of the product by arresting the extension of cracks during high temperature oxidation and corrosion[25].

Table 1 reviews TBC-coated diesel engines and shows how biodiesel affects the engine's performance assessment. Considerable research efforts have been dedicated to LHR engine concept using numerous ceramics coating materials with neat diesel, pure diesel with blends of biodiesel in different proportions to enhance thermal efficiency and to reduce the effluents of CI engine. **Hazar**[26] conduced serious experiments of LHR engine with different TBC materials and fuelled with various sources of feed stocks to determine the performance, burning and effluent characteristics of both layered and unlayered engines. This study reported an enhancement in engine power and reduction in BSFC, with significant reduction in exhaust gas emission and smoke density except increase in NO_x in LHR engine. Zirconium oxide (ZrO_2) has thermally insulating material coated on piston, exhaust and intake valve surfaces provide high power and torque with diminution in exhaust emission and fuel consumption for blends of vegetable oils[27]. The majority of the investigators used yttria stabilized zirconia (YSZ) as TBC material with average thickness of 0.5 mm, in which 400 µm has topcoat and 100 µm has bond coat. The experimental result exhibited a lower fuel economy, with enhanced engine performance and reduction in exhaust emission for LHR engine[28]. However, using cashew net shell liquid, lemon grass oil, kapok oil methyl ester, and leftover cooking palm oil as biodiesel, some researchers carried out a similar experiment on an LHR engine coated with partially stabilized zirconia (PSZ)[29]. It was observed that there was a significant improvement in engine efficiency for the insulated engine. Lanthana-doped YSZ coated LHR engine fuelled with sea lemon methyl esters shows significant progress in thermal efficiency with reduction in exhaust gases, except NO_x[30,31]. **Hazar**[32] developed an LHR engine using chromium carbide (Cr_2C_2) as TBC material in a thickness of 300 µm with Fennel methyl ester blends on single cylinder CI engine and results concluded that partial improvement in exhaust gas temperature (EGT) and thermal efficiency with diminution in exhaust emission, but small increase in NO_x. Further, fly ash coated TBC engine fuelled by 20% volume of rice bran and Pongamia biofuel blended with diesel results in amplifying high-power output, low fuel economy and significant reduction in exhaust emission apart from NO_x.

The reviewed studies reveal consistent improvements in engine performance with TBCs and biodiesel, including increased BTE and EGT, and reduced BSFC. Emission reductions in CO, HC, and SO were common, though often accompanied by increased NO_x. Combustion analyses showed enhanced Combustion Pressure (CP) and Heat Release Rate (HRR), indicating improved thermal efficiency. However, notable research gaps persist, such as limited comparative assessments of coating materials under uniform conditions and inadequate studies on long-term coating durability. These gaps highlight the need for the present study, which uniquely explores the combined effect of TBCs and Scum biodiesel on the performance of a variable compression ratio (VCR) diesel engine.

Engine specification	Coating material/ TBC thickness	Coating technique	Biodiesel source	Performance	Emission	Combustion	Ref.
Engine Type – 1	Molybdenum (Mo)/(300 µm)	Plasma spray	Cotton methyl ester blends (B20 and B40)	BTE:3.5-6% ↑, BSFC: 3.6–5.6% ↓, EGT: 6.2–7.8 ↑	CO: 17–21% ↓, SO: 5.2–8.8% ↓, NO_x: 6.5–7.4% ↑	-	33
BT-140,1 C, 4 s, DI, AC, DE, RP-10 HP @ 3600 rpm, CR 18:1, ECD.	Zirconium dioxide (ZrO_2)	-	Waste corn oil methyl ester blends (B15, B35 and B65)	BTE-↑, BSFC-↓	CO-↓, HC-↓, SO-↓, NO_x-↑ and CO_2-↑	-	34
Engine Type – 2, + RP-4.4 kW @ 1500 rpm, CR 17.5:1,	Partially stabilized zirconia/(500 µm)	Plasma spray	Jatropha oil methyl ester	BTE- ↑, BSFC- ↓	NO_x- ↑	CR- ↑, HRR- ↑	35
Engine Type – 2, + RP-5.2 kW @ 1500 rpm, CR 18:1	Partially stabilized zirconia/(450 µm)	Plasma spray	Waste cooking palm oil biodiesel blends (B10 and B20)	BTE: 0.4% ↑, BSFC: 13% ↓	CO: 22.7% ↓, HC: 24.7% ↓, SO: 10.5% ↓, NO_x: 14.08% ↑	-	29
Engine Type – 2, + RP-3.7 kW @ 1800 rpm, CR 17.5:1	Lanthana (La_2O_3) doped Yttria stabilized zirconia/ (400 µm)	Plasma spray	Methyl esters of sea lemon oil (M20, M40, M60, M80 and M100)	BTE-↑, BSFC-↓, EGT-↑	CO-↓, HC-↓, SO-↓, NO_x-↑	-	31
Engine Type – 1	Chromium(II) carbide (Cr_3C_2)/ (300 µm)	Plasma spray	Fennel seed oil methyl ester (FE30, and FE50)	BTE: 2.08% ↑, EGT: 5.10%↑	CO: 11.09% ↓, HC: 15.64% ↓, SO: 12.82% ↓, NO_x: 12.48% ↑	-	32
Engine Type – 3	Fly Ash/(200 µm)	Plasma spray	Rice Bran and Pongamia biodiesel blends (B20 and B100)	(BTE:2.3–6.8% ↑, BSFC: 6.6–16.8% ↓, EGT: 20.6–27% ↑) * and (BTE:1-4.9% ↑, BSFC: 3.2–13.7% ↓, EGT: 18.3–25% ↑) #	*(HC: 26.4–47% ↓, SO: 35.9–43.2%↓, NO_x: 10.8–26.2% ↑) and (HC: 14.7–41.2% ↓, SO: 33.8–41.9%↓, NO_x: 12.9–28.6% ↑)	CR- ↑, HRR- ↑	36
Engine Type – 1	Aluminum Titanium Oxide (Al_2O_3-TiO_2)/ (300 µm)	Plasma spray	Corn oil biofuel blends (B20, and B100)	BTE: 4.6% ↑, BSFC: 4.7% ↓, EGT: 11.3%↑	CO: 22% ↓, SO: 8.3% ↓, NO_x: 8.8% ↑	-	38
Engine Type – 3	Partially stabilized zirconia/(500 µm)	Plasma spray	Lemongrass oil water emulsion (94% LGO + 5% water + 1% surfactant)	BTE: 1.85% ↑, BSFC: 4.4% ↓	CO: 25% ↓, HC: 10.52% ↓, SO: 15.6% ↓, NO_x: 3.73% ↑, CO_2: 3.03% ↑	CR- ↑, HRR- ↑	41
Engine Type – 2, + RP-7.4 kW @ 1500 rpm, CR 17.5:1	Partially stabilized zirconia/(450 µm)	Plasma spray	Cashew nut shell liquid methyl ester blends (B25)	BTE: 6% ↑, BSFC-↓	CO: 27.7% ↓, HC: 7.2% ↓, SO: 14.3% ↓, NO_x-↑	-	42
				Performance and combustion are improved by using lemon oil biofuel with a cetane booster and TBC. This mixture is even better with a post-treatment system, notably for emission attributes.			
Engine Type – 3	Yttria stabilized zirconia/(500 µm)	Plasma spray	Pine oil with antioxidants such as PO + 1%tertiary-butyl hydroquinone PO + 1% butylated hydroxyl toluene PO + 1% butylated hydroxyl anisole	BTE: ↑, BSFC: ↓	CO: ↓, HC: ↓, SO: ↓, NO_x: ↓	CR- ↑, HRR- ↑	44
				For coated engine with all the three antioxidants used such as: PO + TBHQ, PO + BHT and PO + BHA showed higher performance and combustion characteristics and lower emissions compared to uncoated engines.			
Engine Type – 3	Yttria stabilized zirconia/(500 µm)	Plasma spray	Pomegranate oil methyl ester with different operating conditions such as CR (16.5:1, 17.5:118.5:1and 19.5:1) IT: (19°, 21°, 23° and 25° bTDC) IP: (190–240 bar)	BTE: ↑, BSFC: ↓	CO: ↓, HC: ↓, SO: ↓, NO_x: ↓	CR- ↑, HRR- ↑	45
				Under high engine operating conditions, B20 had better performance, combustion, and emissions.			
Engine Type – 2, + RP-7.4 kW @ 1500 rpm.	Magnesium Zirconate ($MgZrO_3$)/ (500 µm)	Plasma spray	Neem oil methyl ester blends (B10, B15, B20 and B30)	BTE: 11–13% ↑, BSFC: 7–12% ↓	HC-↓, CO-↓, NO_x-↑	-	47
Lambardini 3LD-510,1 C, 4 s, CI, AC, RP-9 kW @ 1800 rpm, CR-17.5:1, ECD.	88%-ZrO_2, 4%-MgO, 8%- Al_2O_3/ (500 µm)	Plasma spray	Waste cooking oil methyl ester blends (B5, and B100)	BTE: 1.33% ↑ BSFC: 4.15% ↓ EGT: 6.04%↑	CO: 6.14% ↓, HC: 13.25% ↓, SO: 16.58% ↓, NO_x: 9% ↑	CP-↑ (2–8 aTDC), HRR-↑ (5-9° bTDC)	48
↑- increase, ↓- decrease, * for Rice Bran oil methyl ester, # for Pongamia oil methyl ester. Engine Type – 1: Lombardini 6LD 400, 1 C, 4 s, DI, AC, DE, RP-6.25 kW @ 3600 rpm, CR 18:1, ECD, Engine Type – 2: Kirloskar, 1 C, 4 s, DI, WC, DE, ECD. Engine Type – 3: Kirloskar-TV1, 1 C, 4 s, CI, WC, DE, RP-5.2 kW @ 1500 rpm, CR 17.5:1, ECD.							

Table 1. Illustrates a review of TBC-coated diesel engine performance, emission, and combustion characteristics under the influence of biodiesel and its blends.

Gaps in knowledge, motivation, aim and novelty

Based on the existing literature, it is evident that many research efforts have investigated the potential of different ceramic based TBCs for diesel engines driven by various ranges of biodiesel sources. These have continuously demonstrated thermal efficiency improvement, reduction in fuel consumption and significant reduction in emissions (CO, HC and smoke distortion) but with an increase in NO_x in the process. However, despite the above developments, an enormous research void still exists in the literature on the utilization of biodiesel from dairy wash water scum as a potential non-edible low-cost bio-waste feedstock that remains largely underutilized.

Furthermore, no studies have been reported on the performance of the present novel biodiesel using optimized engine concepts such as variable compression ratios (VCR) and low heat rejection (LHR) strategies through advanced TBC are conspicuously lacking. This void is important, since scum oil from dairy provides a sustainable alternate route for waste valorization and circular bioeconomy, specifically, in dairy-rich countries, such as India, where disposal of this waste is an environmental concern. In the present study, biodiesel derived from dairy waste scum oil referred to as Scum Oil Methyl Ester (SOME) was evaluated for its suitability in diesel engine applications. However, given the poor fuel properties, direct use of such feedstocks is not possible, so engine modifications are required. In view of this gap, the present work attempts to systematically explore the cumulative influence of VCR together with mullite ($3Al_2O_3{\cdot}2SiO_2$)-based TBC on the performance, combustion behaviour and emission characteristics of CI engine operating with Scum Oil Methyl Ester (SOME) blends. The present research uniquely focuses on original work to determine the optimum value of CR for enhanced engine characteristics with LHR coatings, while simultaneously addressing emission trade-offs.

The novelty of this work lies in three key aspects:

a) It is one of the first few studies which provides an insight of synergistic effect of VCR and mullite TBC on SOME fueled conditions.
b) It uses various SOME-diesel mixtures (B20 to B100) under controlled experimental conditions.
c) A comparative study of the coated and uncoated engine configurations is performed under different CRs and offers useful information for the practical engine optimization with waste-derived biodiesel.

The experimentation was conducted on a single cylinder 4-stroke water cooled VCR engine (5.2 kW, 1500 rpm) with which eddy current dynamometer was developed with a computer interfacing system. All fuel blends were characterized according to ASTM standards prior to testing. The findings seek to provide insights into the development and operation of cleaner and more efficient waste-derived biofuel containing diesel engines in the future.

Materials and methods

Test sample preparation

The optimization of the transesterification process for synthesizing biodiesel from dairy waste scum, using both homogeneous (NaOH) and heterogeneous (CaO nanoparticle) catalysts as presented in the Fig. 1, was thoroughly detailed in the author's previous research. The Fourier transform infrared spectroscopy (FTIR) results and the physico-chemical properties of scum oil (SO) and scum oil biodiesel were also extensively documented in the author's earlier work[7,10]. In the present study, synthesized scum oil methyl ester was blended with pure diesel fuel in six different ratios: B20 (20% SOME, 80% Diesel), B40 (40% SOME, 60% Diesel), B60 (60% SOME, 40% Diesel), B80 (80% SOME, 20% Diesel), B100 (100% SOME), and D100 (100% Diesel). The blending process involved volumetric measurements, where the appropriate ratios of neat diesel and SOME were mixed in a glass beaker, agitated at 1000 rpm on a magnetic stirrer for about 30 min at atmospheric conditions, and then stored in a desiccator for experimental use. The physical and chemical properties of diesel and diesel-SOME blends, and other studies are tested against ASTM 6751 and EN14214 methods are presented in Table 2. In addition, carbon, hydrogen, and oxygen (C/H/O) percentages for SOME and diesel blends were determined using the standard ASTM D5291 method, with the results tabulated in Table 2.

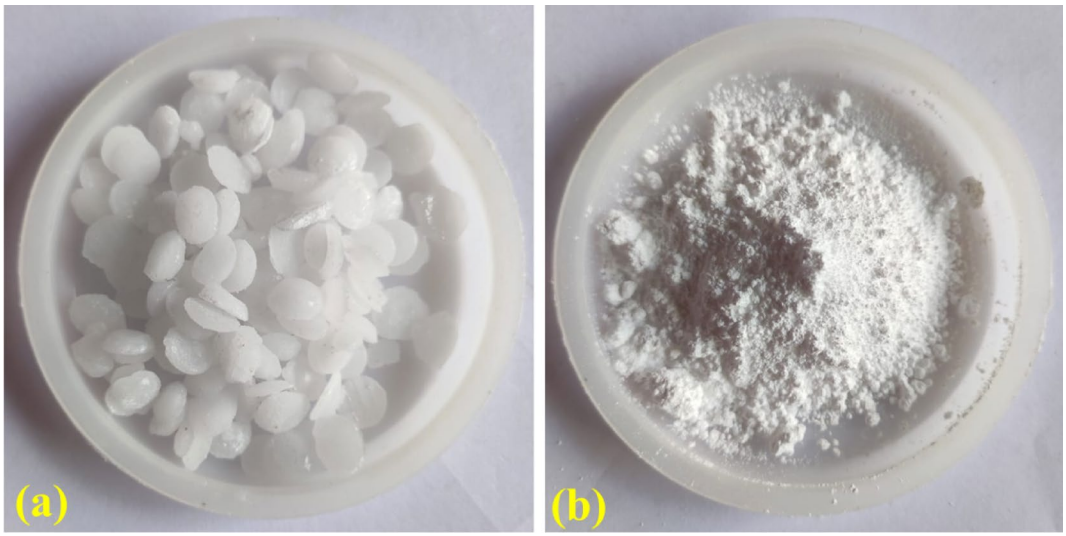

Fig. 1. Visual representation of the catalyst utilized in this study: (a) homogeneous catalyst-sodium hydroxide (NaOH) pellets; (b) heterogeneous catalyst-calcium oxide (CaO) nanoparticles.

Properties	Units	Diesel	B20	B40	B60	B80	B100	MOME[a] [40]	PSOME[b] [49]	LOME[c] [43]	POME[d] [45]
Density at 15 °C	kg/m³	840	846	852	858	864	870	859.3	897.35	848.57	886
Kinematic Viscosity at 40 °C	mm²/s	3.72	3.756	3.792	3.828	3.864	3.9	5.04	5.9	1.02	4.38
Calorific Value	MJ/kg	42.500	42.263	42.027	41.790	41.554	41.317	40.5	40.06	42.76	40.327
Flash Point	°C	50	67.2	84.4	101.6	118.8	136	150.1	192.5	48	126
Cloud Point	°C	−7	−5	−3	−1	1	3	8	12	-	-
Pour Point	°C	−15	−12.2	−9.4	−6.6	−3.8	−1	6	11	-	-
Cetane Number		49.7	51.46	53.22	54.98	56.74	58.5	56	54	52	56.72
Carbon	mass %	86.51	84.52	82.54	80.55	78.56	76.58	76.32	75.69	88.62	76.14
Hydrogen	mass %	13.82	13.61	13.41	13.202	12.99	12.79	12.21	13.98	9.87	13.01
Oxygen	mass %	-	1.87	4.05	6.248	8.45	10.63	11.46	10.33	1.51	10.26
C/H		6.25	6.21	6.15	6.1	6.05	5.98	6.25	5.41	8.97	5.85

Table 2. Physical properties of SOME blends with diesel. [a]MOME = *Moringa oleifera* oil methyl ester, [b]PSOME = Pumpkin seed oil methyl ester, [c]LOME = Lemon oil methyl ester, [d]POME = Pomegranate oil methyl ester.

Parameters	Topcoat mullite ($3Al_2O_3.2SiO_2$)	Bond coat (NiCrAl)
Current (I), A	500	600
Voltage (V), V	55	60
Power, kW	17.5	22.5
Primary gas flow (Argon), L/min	40	40
Secondary gas flow (Hydrogen), L/min	0.8	0.2
Carrier gas flow rate (Ar), L/min	8	10
Powder feed rate, g/min	30	40
Spray distance, mm	100	120
Injector angle, Deg.	90	90
Gun speed, m/s	0.6	0.8
Injector diameter, mm	2	2
Injector distance from torch centerline axis, mm	5	5
Turn table speed, rad/s	50	50
Substrate temperature after coating, °C	128	94

Table 3. Plasma spraying parameters.

Thermal barrier coating by plasma spraying using mullite

The combustion elements such cylinder head, piston crown, inlet and exhaust valves were selected for thermal barrier coating using mullite ($3Al_2O_3$–$3SiO_2$) in this mono cylinder VCR diesel engine experiment. Mullite is the most suitable ceramic material for coating in LHR engines, due to its low thermal conductivity, and excellent physical and mechanical properties. Moreover, mullite's octahedral face is extremely stable and prevents thermal cracks from forming at higher temperatures. Mullite's physical and chemical characteristics are presented in the published literature[50]. The optimum thickness of mullite coating on engine component should be a maximum of 500 µm (0.5 mm). In TBC two layers of coating are done, one topcoat using mullite material and bond coat of NiCrAl (Ni: 22%, Cr: 11% and Al: 67%). This bond coating will protect the slow growth of oxide layer and can accommodate the thermal dissimilarities between the mullite coating and the engine substrate. Also, improves adhesion strength, microstructure, physical and chemical bonding between the ceramic topcoat and engine components[46,51]. Initially, meticulous attention was given to maintaining the same compression ratio and dimensions for the coated piston crown, cylinder head, and valves. This was accomplished by grit blasting the top surface of the engine components to remove a layer of 500 µm until the surface roughness was 4 µm[39]. Anhydrous ethylene glycol was used to ultrasonically clean the engine surfaces after grit blasting and material removal, and the surfaces were subsequently dried. This process ensured that the original dimensions of the coated engine matched the catalog specifications. Table 3 details the plasma spraying parameters. For TBC, the engine components were secured in the holding chuck of the spray booth. Operating under optimized parameters, NiCrAl powder was injected into a high-temperature plasma flame using argon as the carrier gas, resulting in a bond coat layer of 100 µm thickness. This hot molten bond coat impinged on the substrate surface and rapidly cooled to form a bond coating. Subsequently, ceramic powder mullite was sprayed from the plasma torch onto the piston crown, cylinder head, and valve surfaces, forming a topcoat of 400 µm thickness. This process produced a total thermal barrier coating of 500 µm thickness on all engine components. The coating thickness was verified using non-destructive techniques such as calibrated digital thickness gauges, terahertz

(THz) time-domain spectroscopy (TDS), and eddy current testing. Surface roughness was measured using stylus profilometry, wherein a diamond-tipped stylus scans the surface to assess topographical variations, ensuring uniformity and consistency of the coated layer prior to engine testing. The coated piston crown, cylinder head, and valves are photographed in Fig. 2.

Experimental test instrumentation and engine indicating measurement

A computerized variable compression ratio, naturally aspirated, single-cylinder, water-cooled, four-stroke engine integrated with a high-speed data acquisition system was used for this research. The setup included an Eddy current dynamometer, a piezoelectric transducer, a 5-gas exhaust calorimeter, and a smoke analyzer, as shown in the schematic layout in Fig. 3. The engine used was a Kirloskar TV-1 model, with a rated power of 5.2 kW and a constant speed of 1500 rpm. The operating parameters, such as fuel injection timing at 23° bTDC and injection pressure at 200 bar, were set according to the manufacturer's standard values. The engine configuration allowed for modification of the CR by tilting the cylinder block without changing the combustion chamber geometry. Piezoelectric sensors were installed at the cylinder head to measure combustion pressure and fuel line pressure, while an optical crank angle (CA) sensor monitored crankshaft rotation. The system also included components for monitoring airflow, fuel flow, temperatures, and load data. The dynamometer featured strain gauge load cell sensors that sent load signals to a digital load indicator in kilograms. A panel box with an airbox, gasoline tank, manometer, fuel measuring device, transmitters for measuring fuel and air flow, and process indicators were also part of the setup. A 50 cc graded burette and a timer were used to monitor the fuel flow rate volumetrically. A toothed wheel and a magnetic pickup sensor installed on the dynamometer shaft and connected to a frequency meter were used to monitor engine speed. To monitor the steady flow of cooling water to the engine and calorimeter, rotameters were supplied. Six K-type thermocouples were installed to measure exhaust gas, cylinder wall, water inlet, and outlet temperatures. All analog signals from various test setup locations were transmitted to the analysis software "Engines soft 9.0" for engine performance evaluation. Table S-3 provides a detailed outline of the test engine's specifications. The AVL-437 C smoke meter was used to measure exhaust smoke content, with the particle flow opacimeter having a measurement range of 0-99.99% and an accuracy of 0.01 m^{-1}. The AVL-444 DI gas analyzer measured engine exhaust gas emissions. By passing the exhaust gases via a probe, an exhaust gas analyzer can determine the concentrations of CO, CO_2, NO_x, and residual HC. Table S-4 contains precise information on the equipment used to measure engine exhaust emissions.

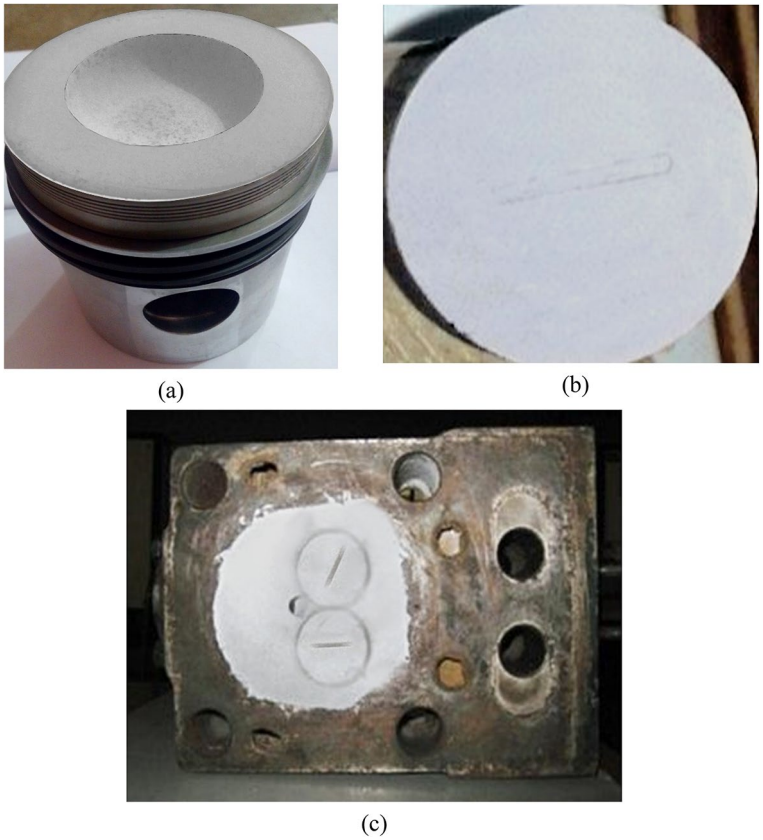

Fig. 2. Photographic view of (**a**) piston Crown, (**b**) valves and (**c**) cylinder head after Mullite coating of diesel engine substrates.

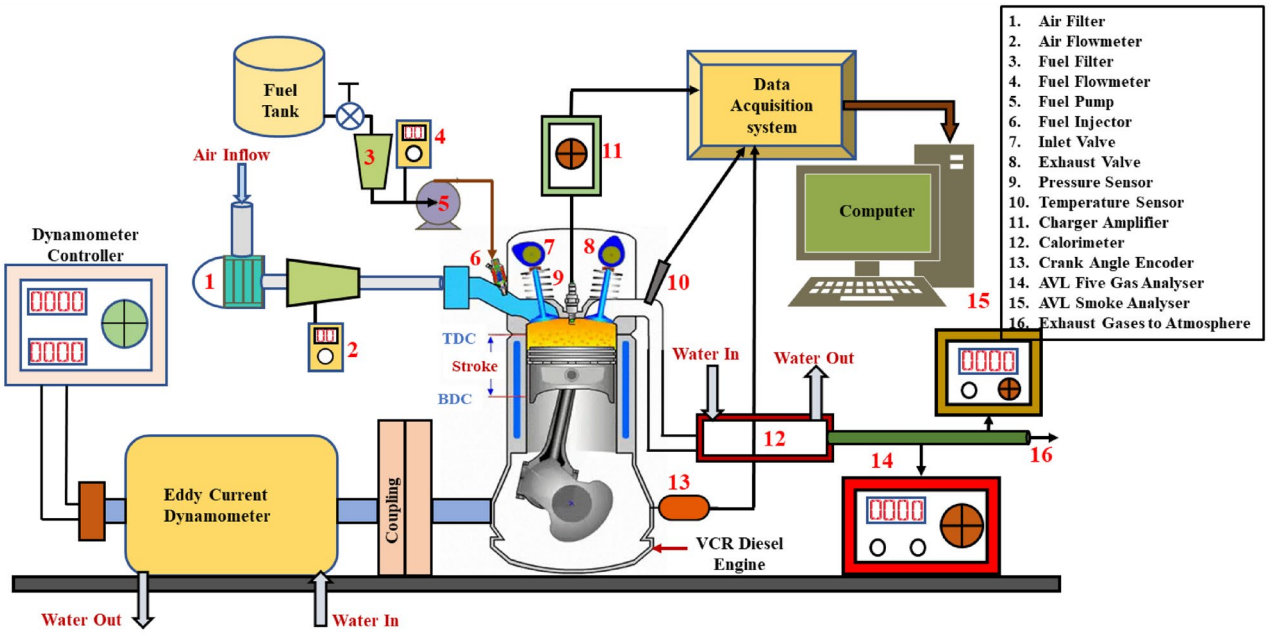

Fig. 3. The schematic diagram of the experimental test setup for the diesel engine.

Measurements	Range	Accuracy	Percentage uncertainties
Gas analyzer	CO_2: 0–20%	± 0.03%	± 0.13
	CO: 0–10%	± 0.02%	± 0.2
	HC: 0-20000 ppm (vol.)	± 10 ppm	± 0.1
	NO_x: 0-6000 ppm (vol.)	± 12 ppm	± 0.2
Smoke measuring instrument	HSU 0-100	± 0.1	± 1
Temperature	0–900 °C	± 1 °C	± 0.15
Speed	0–10,000 rpm	± 10 rpm	± 0.1
Load	0–50 kg	± 0.1 kg	± 0.2
Manometer		± 1 mm	± 1
Pressure pickup	0-110 bar	± 0.1 bar	± 0.1
Burette for fuel measurement	0–100 cc	± 0.1 cc	± 1
Stop watch		± 0.1 s	± 0.2
Crank angle encoder	0–720°CA	± 1°CA	± 0.2

Table 4. Catalog of instruments with their respective ranges, accuracy, and percentage uncertainties.

Experimental procedure and uncertainty analysis

The experimental investigation conducted in the current study has been outlined and summarized in Fig. 4. Diesel and blends of SOME with diesel were used in the performance, combustion, and emission analysis of the VCR diesel engine on both coated and uncoated CI engines. A series of tests were carried out at different loading conditions such as (0, 25%, 50%, 75% and 100%) and at variable compression ratio (16, 17.5 and 19) by maintaining constant speed a 1500 rpm. In the present study three CRs are selected in which 17.5:1 is the standard compression ratio as specified by the manufacture. In order to know how different samples of biodiesel behave at low compression ratio 16:1 has been selected and for higher performance of SOME blend's high compression ratio of 19:1 have been used. In this study, the modification in compression ratio was achieved smoothly, without the requirement to stop the engine or make any modifications to the geometry of the combustion chamber. This was accomplished by implementing a specifically designed configuration of a tilting cylinder block. The variation of CR was performed by setting constant engine speed and with no load conditions. The alignment of the cylinder block and engine basement was achieved by adjusting the lock nut with the aid of eight allen key bolts located on the sidewalls of the cylinder block. The CR of the diesel engine was measured by utilizing a modified screw gauge setup integrated within the engine. Different blend percentages of SOME such as B20, B40, B60, B80, B100 and diesel were used as engine fuel in both LHR and uncoated engine.

The uncoated engine was first operated with diesel at half load condition for 30 min in order to obtain the baseline measurements. The flow rate of both water and fuel has been inspected for engine safety operation. A

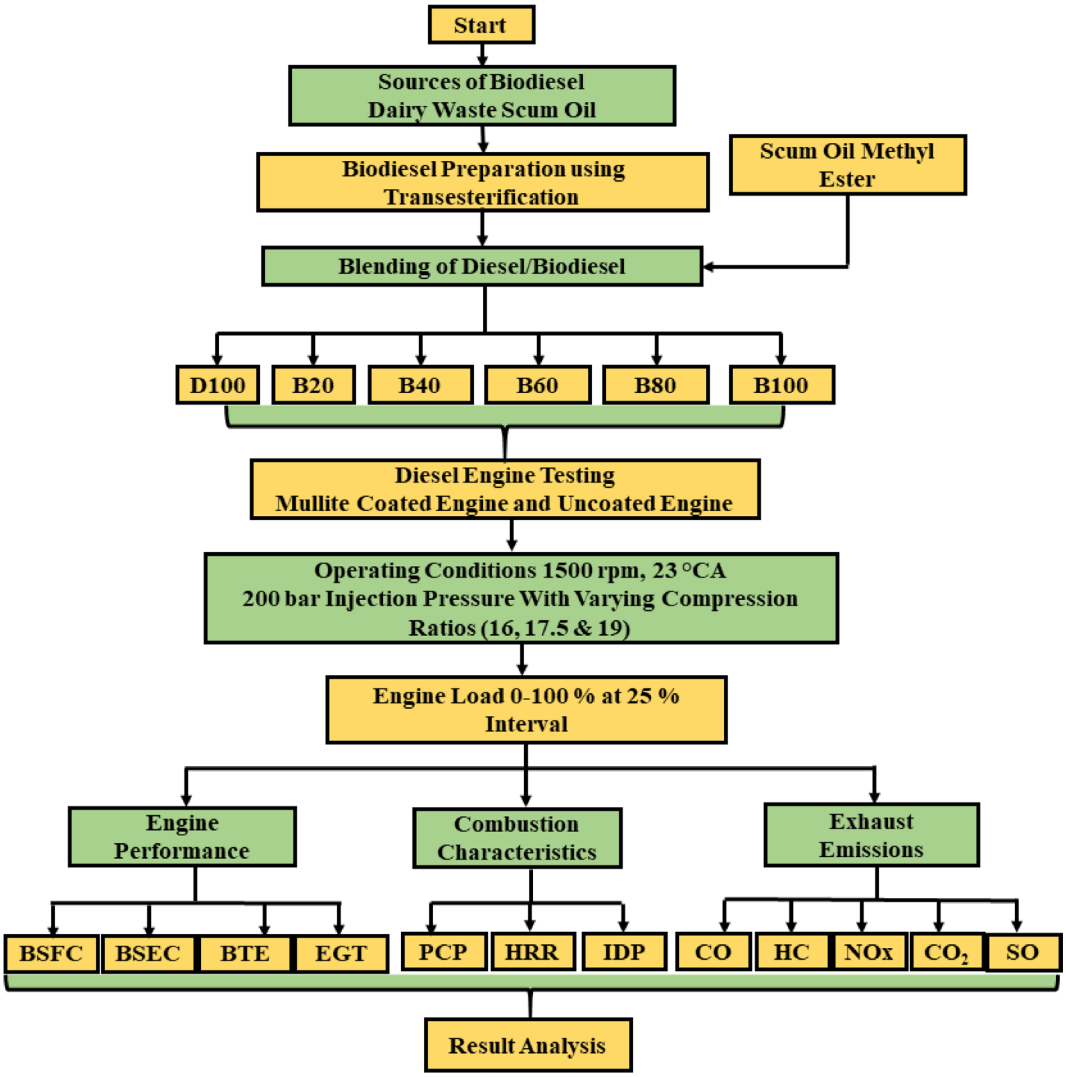

Fig. 4. The flowchart illustrates the experimental testing procedure.

rise in emission temperature to 60–70 °C acknowledged the stable state condition. Pure diesel was used as the threshold fuel for the engine measurements, which were taken from zero load to maximum load. Uncoated CI engine characteristics of neat diesel fuel at different loading conditions and varying CRs were recorded. Similarly, uncoated engine characteristics were measured for different SOME blends with diesel fuel followed by same procedure. After completion of each test the unused fuel sample in the engine unit should be drained completely to fill the tank with a new prepared sample. The components of the combustion chamber, such as the piston, cylinder head, and intake/exhaust valves, were replaced with components that had been coated with mullite. An equivalent experimental investigation was carried out utilizing an LHR engine powered by diesel and different mixtures of SOME at different CRs, and the performance data of the engine were recorded. Obtained results of performance, combustion and emission parameters of both uncoated and coated engines were compared for all the test samples at all CRs with different engine loads. The flow chart of the working principle of VCR diesel engine experimentation has been demonstrated in Fig. 5. However, for all the test samples the engine was operated approximately for 10 min and last 3 min at steady operating conditions data recording has been done. To enhance the trustworthy of quality of results obtained, each engine test was carried out in triplicate with all the test samples in both surface treated and untreated engine and mean values are recorded for further proceedings. All the engine tests were done on the same day so that the recordings would be more accurate and so that the results wouldn't change from day to day as the weather changed. Temperature and humidity are the two things in the air that affect the experiment's work.

The apparent HRR was calculated from cylinder pressure data to estimate the rise in engine cylinder's internal energy during combustion based on the first law of thermodynamics. The HRR value produced during combustion was derived by combining the engine's net HRR, which converts mechanical work corresponding to the CA, with the heat absorbed by the cylinder wall[52]. Following the methodology of Krieger and Borman[44,53], the HRR was determined using Eq. (1) in accordance with the first law of thermodynamics as follows:

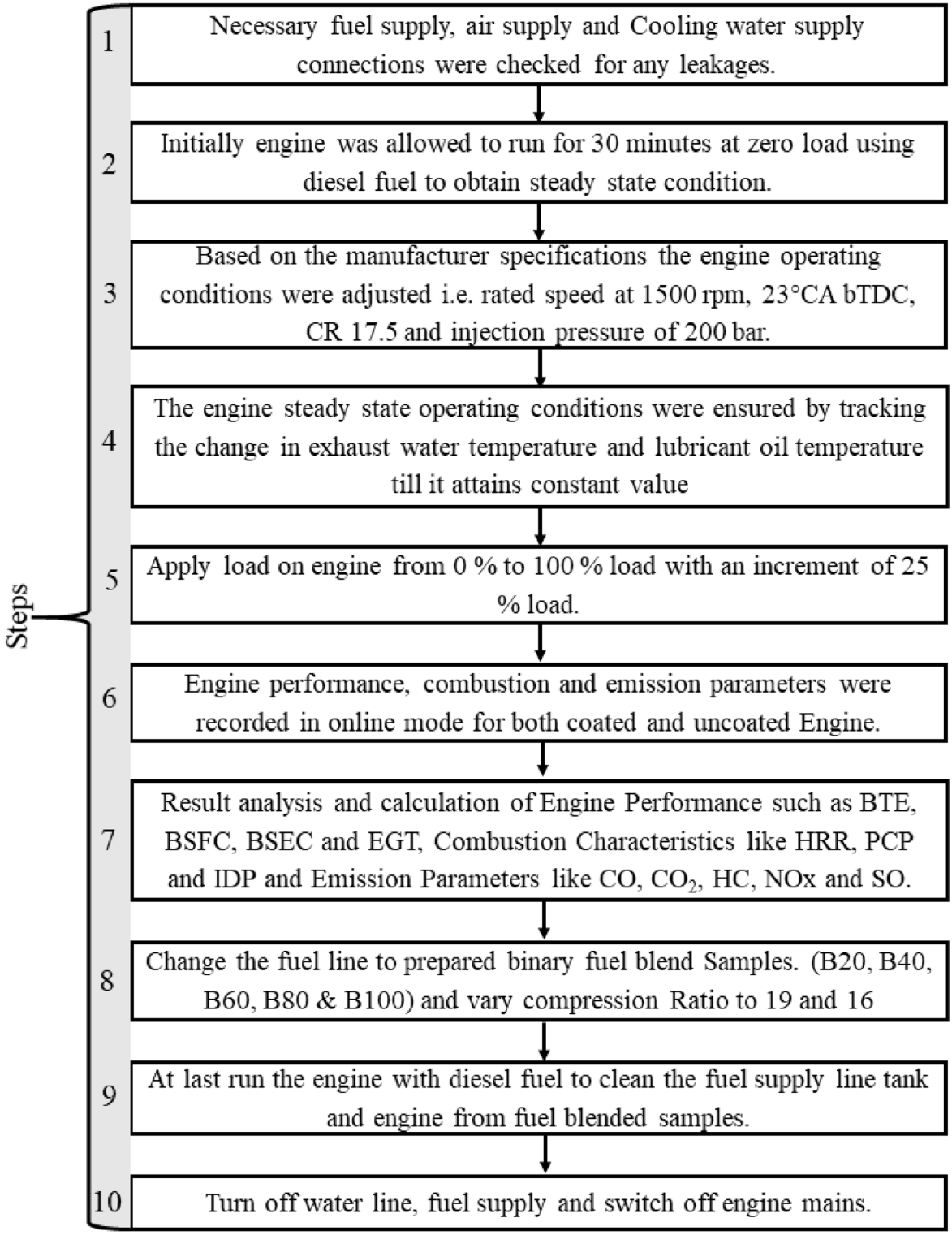

Fig. 5. The flow chart of working principle of VCR diesel engine experimentation.

$$\frac{dQ_{net}}{d\theta} = \frac{\gamma}{1-\gamma} P \frac{dV}{d\theta} + \frac{1}{\gamma - 1} V \frac{dP}{d\theta} \tag{1}$$

where, P: In-cylinder pressure in bar, V: Cylinder volume in m^3, γ: Specific heat ratio, $\gamma = \frac{C_p}{C_v}$, C_p: specific heat at constant pressure, J/kg °C, C_V: specific heat at constant volume, J/kg °C, θ: CA rotation in degree, Q_{net}: Net heat release in J. These emissions can be converted into brake-specific emissions using Eqs. (2–5)[53,54].

$$CO\left(\frac{g}{kWh}\right) = 3.6 \times 10^{-3} \times CO\ (PPM) \tag{2}$$

$$NO_X\left(\frac{g}{kWh}\right) = 6.636 \times 10^{-3} \times NO_X\ (PPM) \tag{3}$$

$$HC\left(\frac{g}{kWh}\right) = 2.002 \times 10^{-3} \times HC\ (PPM) \tag{4}$$

$$CO_2\left(\frac{g}{kWh}\right) = 63.47 \times 10^{-3} \times CO_2\ (Vol.\%) \tag{5}$$

Uncertainties and discrepancies in experimental measurements can arise from factors such as instrument selection, calibration conditions, observation techniques, environmental influences, test planning, and reading accuracy. Despite careful handling, instrument errors are inevitable in all experiments. Therefore, certain uncertainties associated with the measurement instruments are unavoidable and are illustrated in Table 4. Uncertainty (U) analysis is conducted to validate the precision of the experiments. The discrepancies in the results correspond to the maximum error in any variables used for the calculations. In this research, a sample calculation of error/uncertainty is provided in the supplementary material. Using the percentage uncertainties of the various measuring instruments used in the study, total uncertainty (TU) of various variables, including shaft power, brake specific fuel consumption (BSFC), total fuel consumption (TFC), brake thermal efficiency (BTE), CO, CO_2, NO_x, HC, and smoke opacity emission, was calculated. The method of error propagation was utilized to calculate the total percentage uncertainty of an experiment, following Holman's approach. The calculated total percentage uncertainty is ± 2.193%, as derived from Eq. 6, shown below.

$$TU = \sqrt{\left[U_{TFC}^2 + U_{BP}^2 + U_{SFC}^2 + U_{BTE}^2 + U_{HC}^2 + U_{CO}^2 + U_{NO_X}^2 + U_{Smoke}^2 + U_{CO_2}^2 + U_{\substack{\text{Pressure}\\\text{pickup}}}^2 + U_{\substack{EGT\\\text{Indicator}}}^2\right]} \tag{6}$$

$$TU = \sqrt{[1^2 + 0.2^2 + 0.8^2 + 1^2 + 0.1^2 + 0.2^2 + 0.2^2 + 1^2 + 0.13^2 + 1^2 + 0.15^2]}$$

Total percentage of uncertainty = ± **2.193%**.

Results and discussions

Performance characteristics of engine with and without coating

Brake thermal efficiency [BTE

The ratio of an engine's output power to its chemical energy input from the fuel and air supply is known as its thermal efficiency. BTE also considers combustion efficiency, highlighting that not all the chemical energy of the fuel is transformed into heat energy during combustion. Figure 6(a–f) depict the variations in BTE at different CRs (16, 17.5, and 19 CR) for diesel and various blends. The analysis examines the increase in load for engines with both coated and uncoated components. The findings show that BTE progressively rises with increasing load for both diesel and SOME blends in Uncoated Engine (UCE) and Thermal Barrier Coated Engine (TBCE), due to increased fuel supply and decreased heat loss. At first, it was found that thermal efficiency remained similar to diesel when the amount of biodiesel in the fuel mixture was reduced. However, as the blend percentage of SOME exceeds 30% by volume, BTE consistently decreases under all load conditions compared to diesel. This trend is due to inadequate atomization, reduced vaporization, and suboptimal combustion caused by the higher density, viscosity, and lower volatility of SOME[3]. As illustrated in Fig. 6(a–c), increasing the engine's compression ratio is associated with higher BTE for all tested fuels. This aligns with the principle that BTE tends to increase with compression ratio, as supported by previous research. When the CR increased from 16 to 17.5, the average BTE rise by 3.63%, 3.45%, 2.85%, 2.33%, 1.51%, and 3.66%, and when increased from 17.5 to 19, the average BTE increased by 6.38%, 6.67%, 4.01%, 3.49%, 3.45%, and 6.61% for 20%, 40%, 60%, 80%, and 100% of various biodiesel blend ratios and diesel, respectively, under operating load. Higher peak pressure, higher ID, and higher burning temperature are the causes of this improvement in BTE at higher CRs. At CR-19, the BTE for the B20 blend of SOME is the highest among all biodiesel blend samples, being only 0.307% less than pure diesel at maximum loading conditions[55]. Vijay Kumar et al. found that applying a 0.5 mm $3Al_2O_3$–$2SiO_2$ TBC in an LHR engine using Mahua Methyl Ester improved BTE by 13.65% at 25% load, enhanced SFC and BTE at full load, and reduced exhaust temperature, smoke, HC, and marginally CO emissions across all operating conditions[13]. Samuelraj et al. reported that Blend E, containing carbon black, n-pentanol, and soybean biodiesel, improved BTE by 4.90% and reduced BSFC by 25.31% at peak load in an LHR engine. CO, HC, NO_x, and smoke emissions dropped significantly, while in-cylinder pressure and heat release rate increased by 4.52% and 8.87%, respectively, indicating enhanced combustion[12]. As shown in Fig. 6(d–f), BTE is higher for all test fuels in the mullite-coated engine compared to the uncoated engine at all investigated CRs. The mullite coating, with its low thermal conductivity, acts as an insulator, reducing heat loss to the coolant and surroundings, leading to more homogeneous combustion. As thermal energy accumulates in the combustion chamber, the temperature of the gas inside the cylinder and the cylinder walls rises, enhancing combustion efficiency and increasing BTE. Experimental results show that at maximum load, the BTE for the TBC-coated engine increases by 5.49%, 4.08%, 4.01%, 3.17%, 2.78%, and 6.4% at CR 17.5 and by 5.75%, 4%, 3.94%, 2.98%, 2.4%, and 7.51% at CR 19 for B20, B40, B60, B80, B100, and diesel, respectively, compared to the uncoated engine, as shown in Figure S-1. Various literature studies on biodiesel such as Rice Bran, Pongamia, Cashew Nutshell, Rubber Seed, Cotton Seed, Neem Kernel Oil, and Frying Oil used in TBC-coated engines reported an increase in BTE between 3.8% and 8.3%[49].

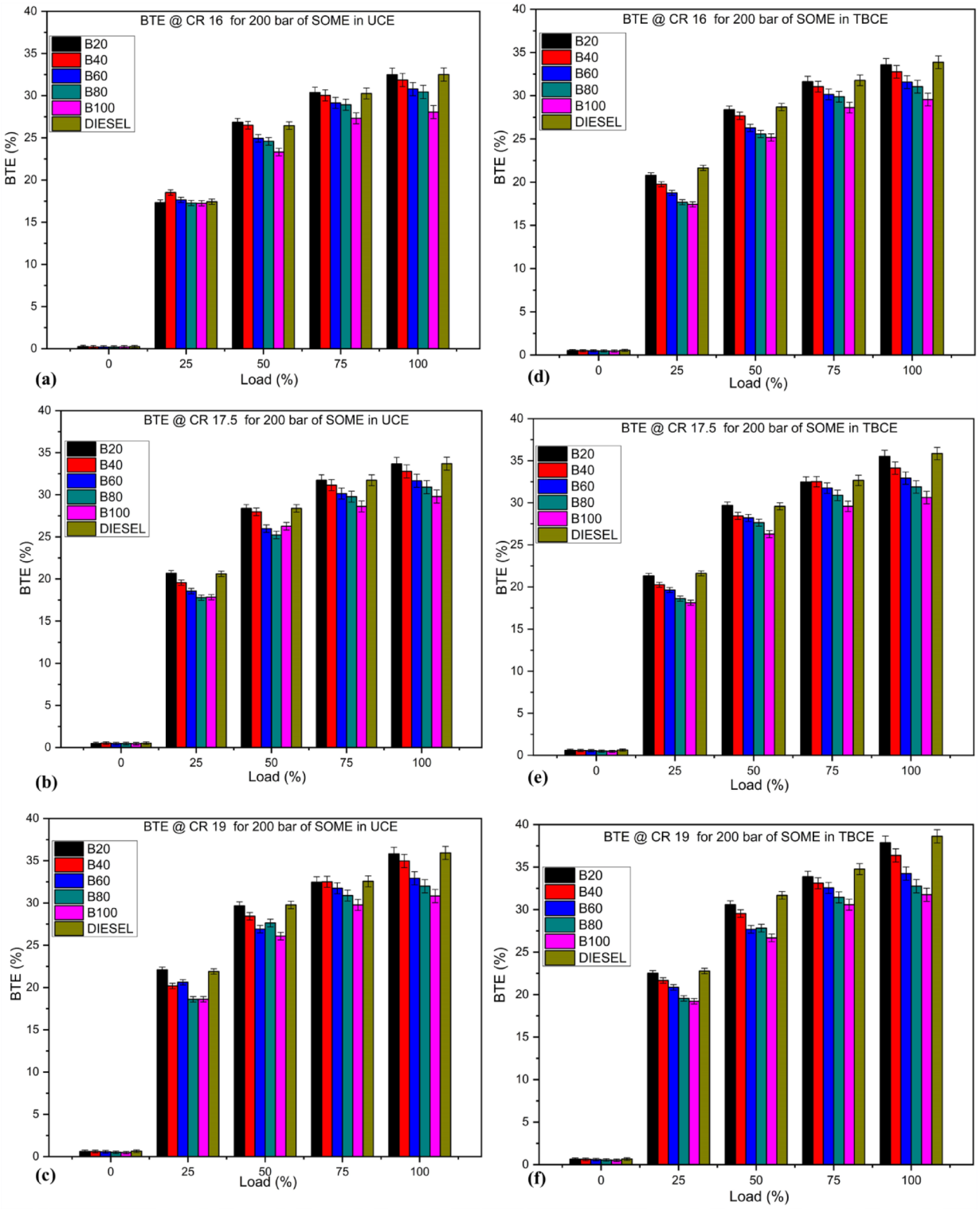

Fig. 6. (**a**–**f**) The variation of the BTE at various loads and CRs (16, 17.5 & 19) for SOME blends in both coated and uncoated engines.

Brake specific fuel consumption

During engine testing, fuel consumption is measured by the rate at which fuel is consumed, expressed as the mass of fuel per unit of time. BSFC measures the amount of fuel used (in g/h) to produce one unit of power (kW) and is inversely related to BTE. Figure 7(a–f) shows the variation of BSFC for both surface-treated and untreated diesel engines fueled with diesel and blends of SOME, under varying load conditions and CRs. BSFC decreases with an increase in load and CR for all samples in the uncoated engine. BSFC experiences a significant

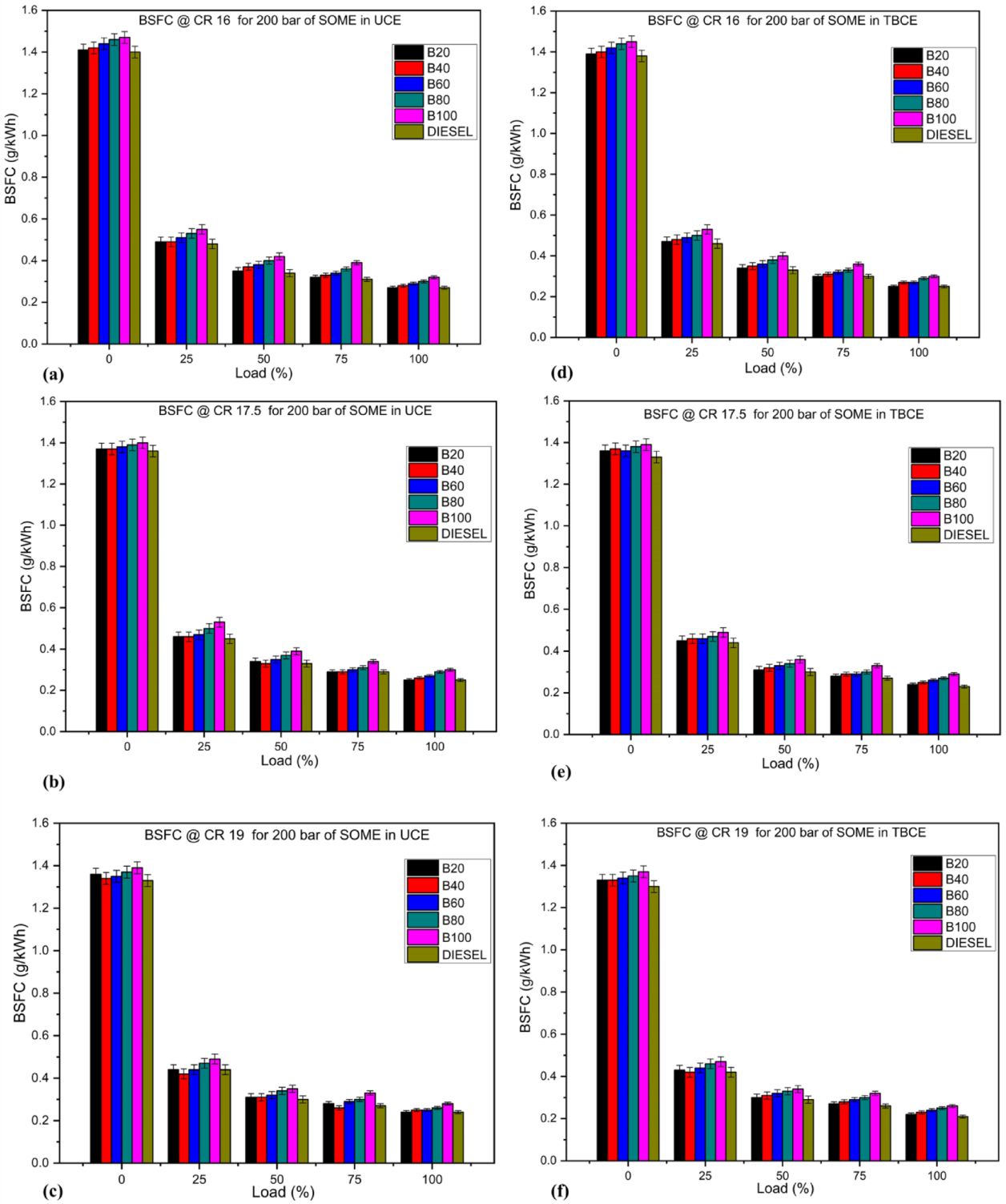

Fig. 7. (**a–f**) The variation of the BSFC at different loads and CRs (16, 17.5 & 19) for SOME blends in both coated and uncoated engines.

60% reduction from no load to quarter load, with a slight decline noted at 25% load. Due to the reduced calorific value at higher blend percentages, biodiesel blends have slightly higher BSFC than pure diesel. Consequently, more fuel is required for combustion to produce 1 kW, leading to an increase in BSFC[56,57]. Biodiesel blends with proportions of 20%, 40%, 60%, 80%, and 100% in the uncoated engine showed an 8%, 7.69%, 7.41%, 3.44%, 6.66%, and 8% decrease in BSFC when the CR varied from 16 to 17.5, and a 4.17%, 4%, 8%, 11.53%, 7.14%, and 4.17% decrease in BSFC when the CR varied from 17.5 to 19, respectively (Fig. 7(a–c)). Increasing the CR leads

to a decrease in BSFC for all samples, likely due to reduced ID and improved conversion of heat to mechanical work, resulting in smoother engine operation. The results indicate that biodiesel shows a better decrease in BSFC than diesel as the compression ratio increases, attributed to the lower volatility and higher cetane number of biodiesels, which enhance combustion at higher CRs compared to diesel[45].

The variation of BSFC for the mullite-coated diesel engine at varying loads for all test samples and CRs is displayed in Fig. 7(d–f). For all test samples, mullite-coated engines had lower BSFC than the uncoated engine across all CRs and engine load. Improved heat retention in the combustion chamber raises in-cylinder gas and wall temperatures, which improves fuel burning due to heat insulation in the coated condition. The ID period lowers as LHR engine cylinder and wall temperatures rise, improving fuel atomization and air-fuel blending. Consequently, the improved combustion conditions favor reduced amounts of test fuel, positively affecting both physical and chemical delays. Comparing the coated engine to the conventional diesel engine, this causes a drop in BSFC for all test samples at different CRs. For B20, B40, B60, B80, B100, and diesel in the coated engine, BSFC decreases by 4.7%, 4%, 3.84%, 7.84%, 3.44%, and 8.69% at CR-17.5, and by 9.09%, 8.69%, 4.17%, 4%, 7.69%, and 14.28% at CR-19, respectively, compared to the uncoated engine, as depicted in Figure S-2[58]. In this study, the BSFC reduction reached up to 9.09% for B20 blend and 14.28% for diesel in the TBC engine, which is consistent with the reductions reported by (6.5%)[43]. The observed BSFC improvement is notably higher than that reported by Soudagar et al.[59](3.5–5.6%) and contrasts with Muralidharan et al.[60], who observed an increase of 9–10% in BSFC with biodiesel blends. These improvements in the present study can be attributed to the synergistic effects of the optimized compression ratio, enhanced combustion due to the mullite thermal barrier coating, and the favorable fuel properties of scum oil methyl ester. Various studies have reported a significant improvement of around 4.8% in LHR engines using different biodiesels, which is consistent with the findings of the current study[32].

Brake specific energy consumption (BSEC)

BSEC is defined as the metric that quantifies the efficient energy produced from the combustion of fuel to generate unit brake power within a specific timeframe. The determination of BSEC is a more realistic parameter compared to BSFC for assessing the performance of a CI engine running on various test samples with different densities and lower heating values[45]. BSEC is typically calculated as the product of the fuel's lower heating value and BSFC, as shown in Eq. (7).

$$BSEC = Low\ calorific\ value\ \times\ BSFC \tag{7}$$

Figure 8(a-f) illustrates the variation in BSEC values for both uncoated and mullite-coated VCR engines fueled with diesel and SOME blends at different CRs under varying loads. Essentially, BSEC decreases with an increase in load and CR, mirroring the trends observed in the BSFC figures for all tested fuel samples. From Figs. 9(a-f), it is evident that conventional diesel fuel has a lower BSEC than all biodiesel blend samples across different engine loads. However, B100 shows the highest BSEC value among the biodiesel samples due to its higher BSFC, lower calorific value, longer ID, higher flash point temperature, and poorer atomization properties[43]. Under peak engine load conditions, the average decrease in BSEC was 8.05%, 7.87%, 7.44%, 3.48%, 6.69%, and 7.99% when CR increased from 16 to 17.5, and similarly, the average decrease in BSEC was 3.13%, 3.8%, 8.05%, 11.57%, 7.09%, and 4.22% when CR increased from 17.5 to 19 for B20, B40, B60, B80, B100, and diesel, respectively, in the uncoated diesel engine, as shown in the BSEC graphs. The results indicate that increasing the compression ratio (CR) leads to a consistent reduction in Brake Specific Energy Consumption (BSEC) across all fuel samples, primarily due to enhanced thermal efficiency and shorter ignition delay, contributing to smoother engine operation. Fuel consumption showed a notable dependency on CR under varying engine conditions, directly influencing BSEC values. CR 17.5 served as the reference operating condition, while a further increase to CR 19 resulted in lower fuel consumption, likely due to improved combustion efficiency and optimized in-cylinder thermodynamic conditions, despite slightly reduced air availability from altered cylinder volume. In contrast, at CR 16, higher volumes of both fuel and air were required to maintain the rated power output, indicating suboptimal combustion. Interestingly, as shown in Fig. 8(c), BSEC values for B20 closely matched those of diesel at higher CRs, attributed to reduced fuel usage driven by better Brake Thermal Efficiency (BTE) and superior fuel–air mixing characteristics[61].

Figure 8(d-f) describes the variation in BSEC for the LHR diesel engine at different CRs and varying loads for various fuel samples. The graphs show that BSEC decreases for the mullite-coated engine compared to the uncoated engine as engine load and CRs increase for all test samples. This is attributed to higher combustion chamber temperatures, improved fuel atomization, reduced ID, enhanced vaporization rate, and lower fuel consumption exhibited by the thermally coated diesel engine. These factors further decrease BSEC at higher CRs for all fuel samples in the thermally coated engine compared to the uncoated CI engine[9,61]. At maximum engine load, BSEC values in the coated engine are 10.14, 10.51, 10.86, 11.22, 11.98, and 9.77 MJ/kWh at CR-17.5, and 9.29, 9.67, 10.03, 10.39, 10.74, and 8.92 MJ/kWh at CR-19 for B20, B40, B60, B80, B100, and diesel, respectively. At 100% engine load, a reduction in BSEC of 4.14%, 3.9%, 3.87%, 7.39%, 3.42%, and 8.8% at CR-17.5 and 10.22%, 8.79%, 4.09%, 3.94%, 7.73%, and 14.35% at CR-19 for B20, B40, B60, B80, B100, and diesel, respectively, was observed in the thermally coated engine compared to the uncoated diesel engine, as shown in Figure S-3. The use of the mullite-coated engine resulted in a significant reduction in BSEC values of 5.25% at CR-17.5 and 8.18% at CR-19 with SOME blends, consistent with the findings of Karthikeyan et al.[45].

Exhaust gas temperature

The exhaust gas temperature (EGT) is a significant measurement that can be used as proxy for combustion quality inside the cylinder and is directly related to the in-cylinder temperature at the time of combustion.

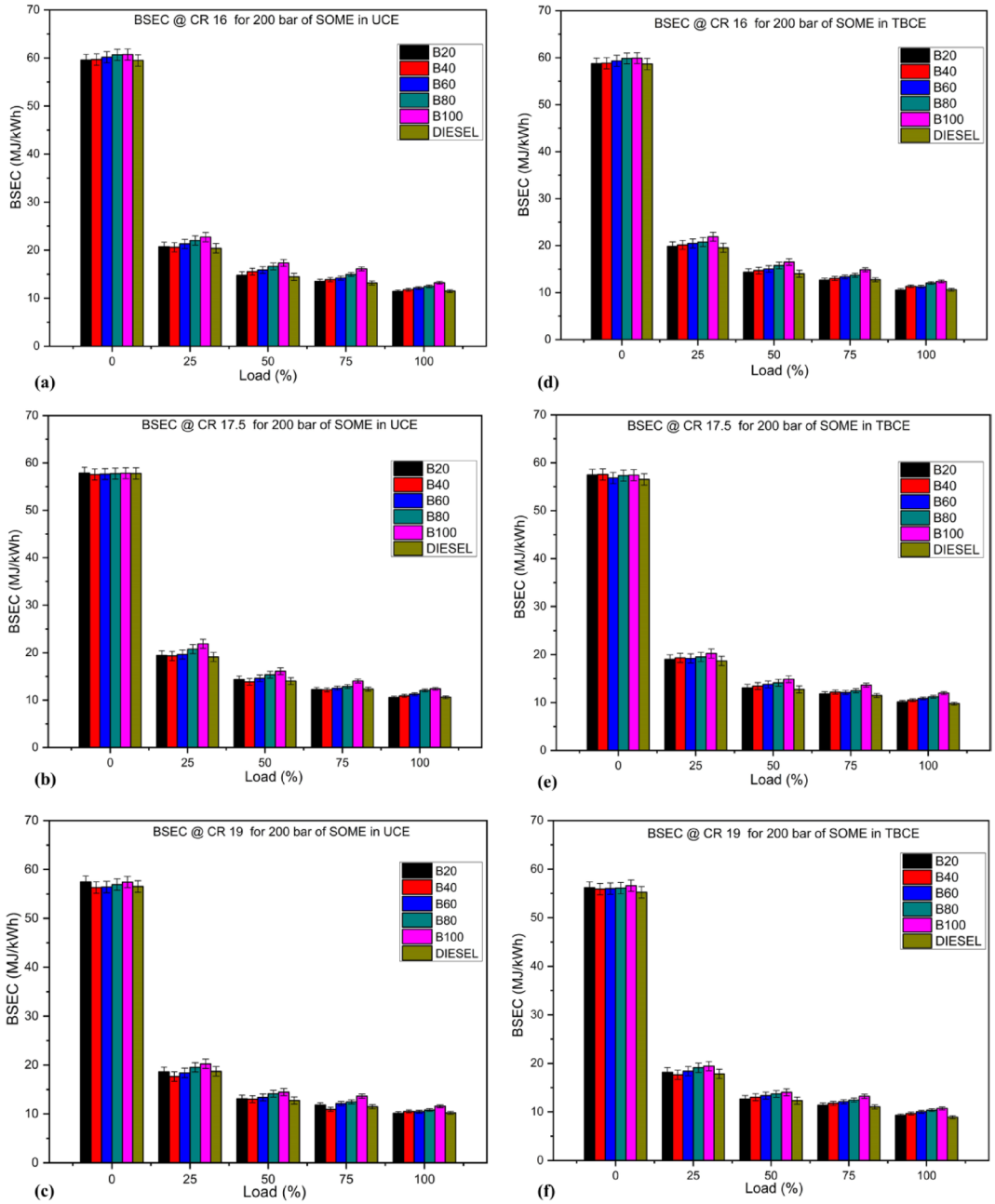

Fig. 8. (**a**–**f**) The variation of the BSEC at various loads and CRs (16, 17.5 & 19) for SOME blends in both coated and uncoated engines.

From Fig. 9(a–f), it is observed that EGT always increases with load for all test fuels and CRs, whether it is in uncoated and LHR diesel engines. This increase is due to a higher load more fuel is injected per unit time, in which heat release is increased to maintain sustain torque output. Nevertheless, blends of higher quantities of SOME biodiesel presented systemically slightly lower EGT than diesel, this tendency was more accentuated at higher CR. This decrease is due to the lower heating value and the higher oxygen content of biodiesel which lead to more complete combustion though at lower peak flame temperatures. At the lowest CR (16:1), in particular, EGT values were higher for all fuels. At 17.5 and 19 CR, EGT values of biodiesel blends are less than those of diesel which gives better thermal efficiency with increased CR[8]. At CR-17.5 EGT for diesel is 368.93 °C, for B20: 363.67 °C and for B100: 344.68 °C. Similarly, at CR-19 EGT for diesel is 363.67 °C, for B20: 360.09 °C and for B100: 342.46 °C, at operating conditions. The decrease in EGT at greater CRs can be ascribed to various variables, such as the reduced calorific value, increased oxygen content, elevated flash point, and diminished end-of-compression temperature of certain mixed fuel in comparison to diesel. The combustion temperature is a critical factor in understanding the generation of NO_x inside the engine cylinder. Performance may increase due to lower exhaust loss[62]. As the CR increases, the volume of EGT at peak load decreases. This is due to improved

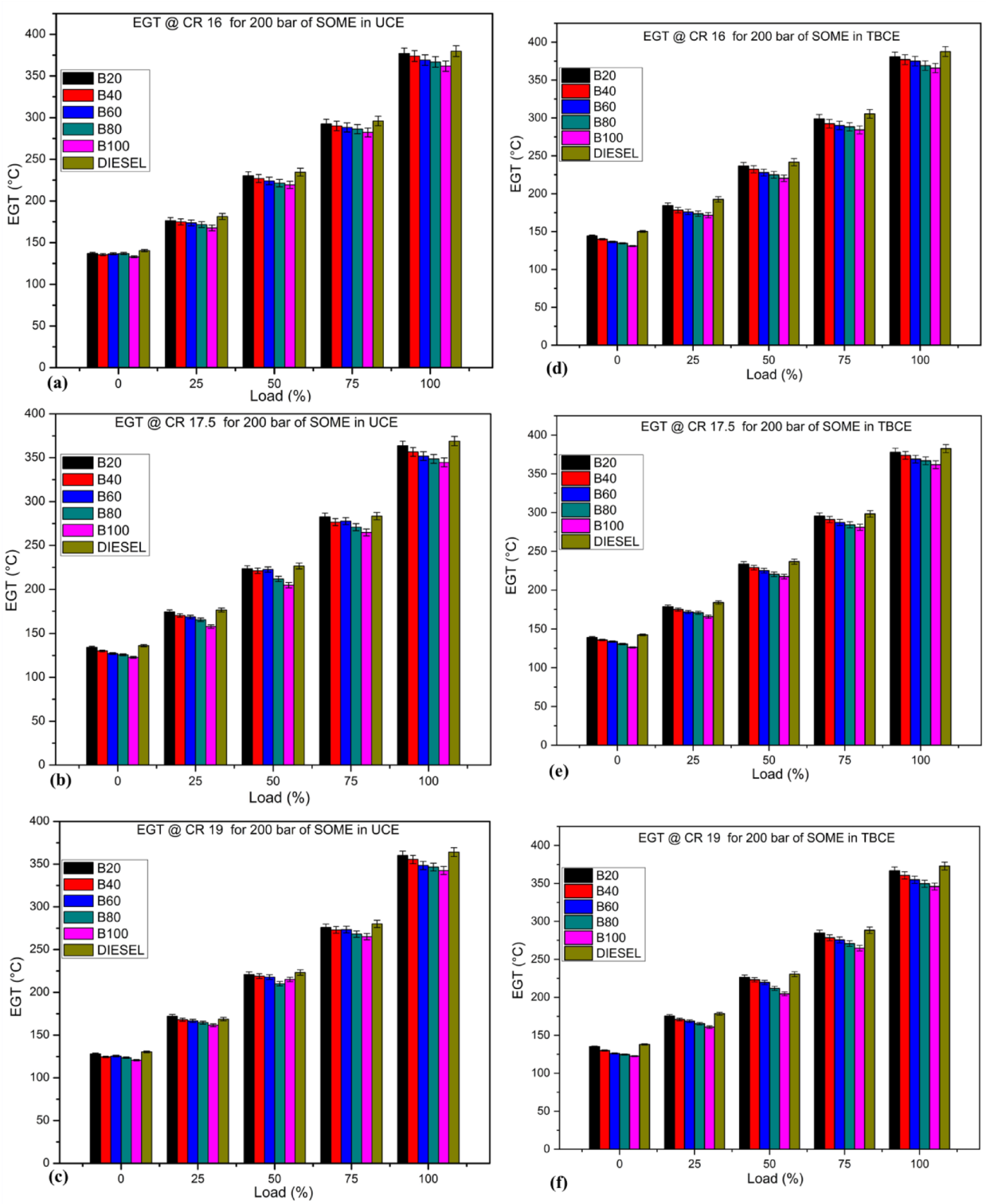

Fig. 9. (**a**–**f**). The variation of the EGT at various loads and CRs (16, 17.5 & 19) for SOME blends in both coated and uncoated engines.

fuel atomization and air-fuel ratio. In comparison of EGT in LHR and uncoated engine, an increase of 3.91%, 4.85%, 4.9%, 5.21%, 4.97% and 3.72% at CR-17.5 and 1.83%, 1.49%, 1.87% 0.93%, 0.99% and 2.47% at CR-19 for B20, B40, B60, B80, B100 and diesel respectively, at peak load condition were determined. According to these results, it is seen that the increase in EGT is more noticeable in LHR engines than uncoated engines, as the loss of heat to the coolant and surroundings decrease significantly in LHR engines. This amount of heat is transferred

to the exhaust gas because TBC can give off maximum temperature[48,63]. The variation of EGT with CRs at peak load for all test samples in both uncoated and TBC engine is shown in Figure S-4.

Combustion characteristics

Combustion cylinder pressure (CCP)

The amount of fuel burned during the premixed combustion phase, the first stage of combustion, has an impact on the CCP in a direct injection diesel engine. The characteristics of cylinder pressure reflect the fuel's ability to mix with air and combust. The combustion process in CI engines consists of two main phases: the premixed phase and the diffusion phase. The premixed phase begins immediately after fuel injection, where the fuel and air mix thoroughly to form a highly flammable mixture before ignition. A critical aspect of this process is the ID, the time interval between the SOI and the SOC. During ignition, this fuel mixture reacts quickly. After the oxygen in this combination is burned, the combustion process enters the diffusion phase, governed by fuel-air mixing[64]. For an optimum TBCE configuration at CR 17.5, pressure rise was early and peak cylinder pressure was advanced compared to UCE, indicating shorter ignition delay due to higher in-cylinder thermal conditions. This thermally promoted shift of combustion phasing increases pressure–temperature coupling and may lead to an increase in thermal efficiency, particularly for biodiesel-enriched blends[53].

The diffusion phase is much longer than the premixed phase[65]. The fluctuations in CCP relative to CA under rated load (100%) conditions for different CRs across various blends of SOME and diesel are depicted in Fig. 10(a-f) for both LHR and uncoated engines. Diesel has a higher peak cylinder pressure than biodiesel at all engine loads and CRs in both uncoated and coated engines. The peak cylinder pressure for B20, B40, B60, B80, B100 and diesel where 72.36 bar, 71.26 bar, 70.76 bar, 69.48 bar, 67.33 bar and 73.54 bar at CR-17.5 and 73.68 bar, 72.79 bar, 72.31 bar, 71.95 bar, 71 bar and 74.94 bar at CR-19 respectively, at crack angle between (7–10°) away from Top Dead Center (TDC) in uncoated engine. Every occurrence of maximum pressure was seen to take place distinctly after the TDC, which indicates that the engine was operating safely and efficiently. Alternatively, if the maximum pressure occurs near or prior to the TDC position, it can result in significant engine knocking, which in turn can negatively impact the longevity of the engine. Diesel has the highest peak pressure than biodiesel blends, because diesel fuel has higher ignition period with lower viscosity and cetane number in which fuel air mixes readily resulting in proper combustion leading to higher cylinder pressure at peak load. Figure S-5(a – f) describes the fluctuation in cylinder pressure with load (0-100%) for different test fuels at varying CRs in both coated and uncoated engine using SOME blends. When CR increased from 16 to 19, biodiesel blends had more benefits than diesel. Because of their low volatility, biodiesel blends have higher viscosity, better atomization, faster mixing of air fuel, and shorter ID due to higher cetane number and oxygen fortification. Additionally, higher peak pressure is caused by less penetration with increased cone angle[66].

For LHR engine peak pressure will be higher at all CRs with rises in load for all the samples when compared to uncoated engine. In TBC, the engine burning starts earlier than for uncoated engines at all engine loads and CRS with a decrease in ignition period and advanced injection timing. Consequently, the maximum cylinder pressure reaches an elevated level for all test fuels and further observed that CA position came very close to TDC in the expansion stroke. The Fig. 10(d – f) shows that peak pressure for TBC engine was recorded to be 73.54 bar, 72.36 bar, 71.26 bar, 70.76 bar, 69.48 bar and 74.55 bar at CR-17.5 and 74.94 bar, 73.87 bar, 72.75 bar, 72.29 bar, 71.95 bar and 76.58 bar at CR-19 for B20, B40, B60, B80, B100 and diesel respectively at 100% load between the CA position (6–8°) after TDC. In TBC engine peak cylinder pressure is measured at the CA between (6–8°) ATDC, but for uncoated engine it is shifted slightly away from TDC (8–10°) for all test fuels and CR at maximum load. In the present work, the TBC engine had presented a higher maximum cylinder pressure of 76.58 bar for diesel, and 74.94 bar for B20 between 6–8° ATDC. This is related to the improving CR and the heat insulation effect caused by the mullite coating, which leads to higher in-cylinder temperature and faster heat release[39]. On the other hand, uncoated engines had the trend of delayed peak pressure (8–10° ATDC). The reduction in ignition delay and improved combustion with SOME blends further support this trend, aligning well with previous findings. Similar improvements have been also reported by the authors earlier during studies on biodiesel in TBC-fitted engine[32].

Heat release rate

The HRR is used to determine the SOC, quantify the amount of fuel burned, and identify variations in the fuel's combustion rate. The cetane number of the fuel indicates its ignition quality; a higher cetane number results in a shorter ID period. The chemical and physical processes occurring during the ID period are generally endothermic, causing the combustion model to exhibit negative heat release during this period, which quickly turns positive upon auto-ignition. After the ID, the pre-mixed air-fuel mixture burns rapidly, producing the first peak in the HRR. Once premixed combustion is completed, the process transitions to the diffusion phase, where the burning rate is maintained by the presence of a combustible mixture[67]. Figure 11(a-f) compares the effects of CR on the HRR with diesel and scum oil biodiesel blends in relation to CA for both TBC and uncoated engine operations. As illustrated in Fig. 11(a–c), with the increase of scum oil biodiesel blend, a shorter ID period occurred than that of diesel. As a result, the maximum rate of heat release during the combustion phase, when fuel and air are mixed, gradually decreases and shifts to earlier points in the engine's rotation. The observed result can be ascribed to the decreased fuel injection quantity during the shorter period between ignition and combustion, as well as the lower energy content of the scum oil biodiesel[68].

It has been observed that the maximum HRR decreases at lower compression ratio and gradually increases at higher compression ratio for all test fuels at max load. However, the peak HRR for convention fuel is larger than that of biodiesel blends at all CRs. This is due to the extended period it takes for the ignition to occur, which leads to a greater buildup of the fuel-air combination within the cylinder. The reduced density and viscosity of diesel fuel enable enhanced fuel mixing and atomization, resulting in a greater rate of heat release. The max HRR are

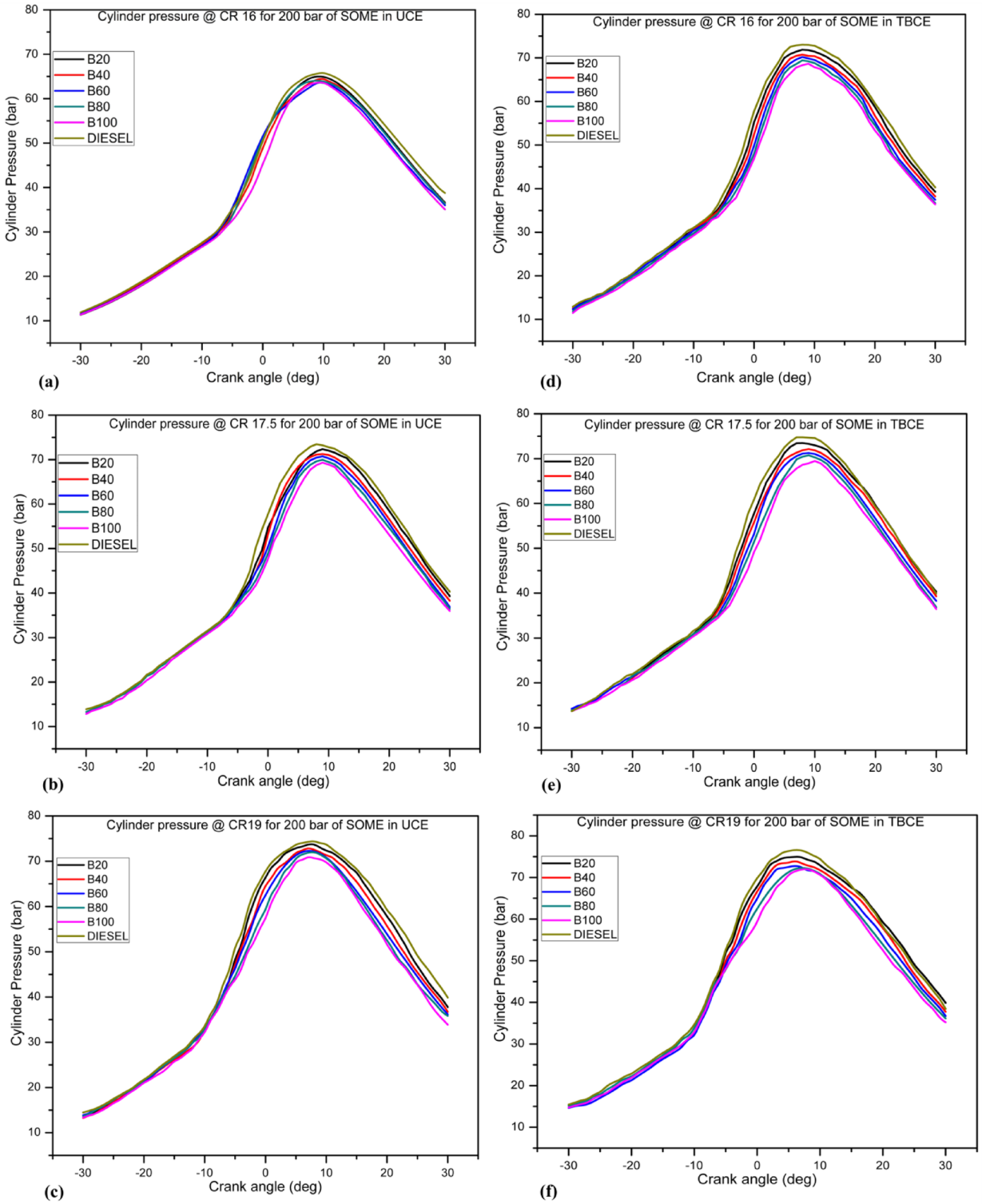

Fig. 10. (**a**–**f**). The variation of cylinder pressure with CA and CRs (16, 17.5 & 19) for SOME blends in both coated and uncoated engines.

46.97, 44.78, 43.12, 39.87, 36.34 and 47.49 J/°CA at CR 17.5 and 45.82, 44.12, 41.85, 41.79, 41.23 and 47.97 J/°CA at CR 19 for B20, B40, B60, B80, B100 and diesel respectively under max load condition in uncoated engine. During peak load, the mullite-coated engine fueled with diesel exceeds SOME mixes in terms of highest HRR, regardless of the CRs. The variation is due to the extended period it takes for diesel fuel to ignite, along with its greater energy content, as well as the higher operating temperature that is typical of engines equipped with TBC.

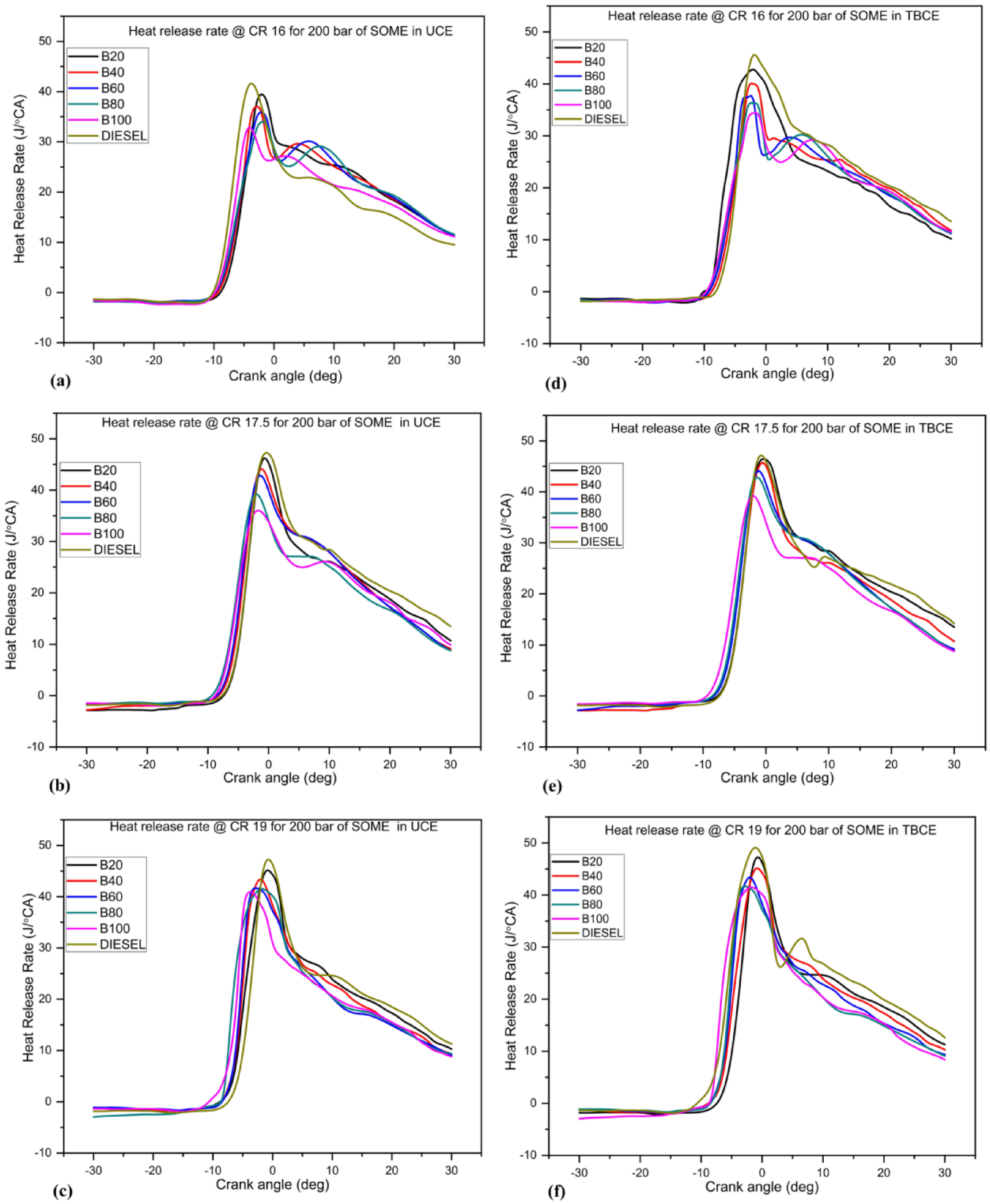

Fig. 11. (**a**–**f**). The variation of HRR with CA and CRs (16, 17.5 & 19) for SOME blends in both coated and uncoated engine.

From Fig. 11(d–f) it was noted that at higher engine load, the HRR for coated engine is greater and occurs at a CA very close to TDC i.e., between (2 − 0°) BTDC (before top dead centre). As seen in the graphs the net HRR was marginally higher for coated engines than engines with uncoated, and it increases with rise in compression ratio. In uncoated engine retardation of injection timing increases the ignition period due to which premixed combustion phase is shortened resulting in lower HRR. The max HRR for LHR engines is 46.6, 45.97, 44.78, 43.12, 39.87 and 47.97 J/°CA at CR-17.5 and 48.68, 45.82, 44.12, 41.85, 41.79 and 49.61 J/°CA at CR-19

for B20, B40, B60, B80, B100 and diesel respectively at peak load. In the present study, the maximum HRR in TBC engine was found at 49.61 J/°CA and 48.68 J/°CA for diesel and B20 at a compression ratio 19, respectively. These values are in agreement with the previously reported HRR rise of 4.9–7.8% when coated engines are compared to uncoated[69]. The enhanced HRR and earlier combustion peaks in this study result in better combustion quality (i.e., more efficient combustion), which can be attributed to an optimized compression ratio, lower thermal loss resulting from the mullite coating and the excellent ignition quality of scum oil methyl ester, which collectively facilitate rapid and complete combustion. The combustion span graphs for different biodiesel blends and diesel with different compression ratio for with and without coated engine are illustrated in Figure S-6 (a-f) which is presented in supplementary material.

Combustion parameters

In compression ignition (CI) engines, combustion is typically characterized by key sequential phases: ignition delay (ID), premixed combustion, diffusion combustion, and afterburning. The nature and efficiency of these phases largely depend on the physicochemical properties of the fuel used. In the current study, critical combustion parameters such as start of injection (SOI), start of combustion (SOC), ignition delay (ID), combustion duration (CD), and cumulative heat release rate (CHRR) were systematically evaluated for various blends of Scum Oil Methyl Ester (SOME) and diesel under different compression ratios (CRs) and engine configurations (uncoated and thermal barrier-coated). The determination of SOI was based on a threshold needle lift of 0.01 mm, marking the onset of dynamic fuel injection[70]. The injection delay (IND), defined as the difference between static and dynamic fuel injection timing, and SOC were derived using pressure derivative analysis. The SOC corresponds to the crank angle (CA) at which the second derivative of in-cylinder pressure crosses zero prior to its maximum slope an indicator of rapid combustion initiation[63].

Ignition delay, the interval between SOI and SOC, is a crucial parameter influenced by the fuel cetane number, viscosity, density, and oxygen content. It plays a pivotal role in shaping combustion characteristics such as peak cylinder pressure (PCP), HRR, and SOC timing. In this study, biodiesel blends exhibited moderately delayed SOI compared to diesel, with observed delays of −2.635°CA and − 1.06°CA at CR 16 under full load in uncoated and coated engines, respectively[71]. This delay is primarily due to the higher viscosity and bulk modulus of SOME, leading to increased nozzle pressure and slower fuel response. As CR increased, SOI timing in uncoated engines aligned more closely with the manufacturer specification, deviating only by 0.751°CA at CR 17.5 and − 0.212°CA at CR 19. In contrast, TBC engines showed slight advancement in SOI by 0.766°CA at CR 17.5 and 0.682°CA at CR 19 reflecting the impact of increased cylinder wall temperature and reduced viscosity of biodiesel during injection. The higher cetane number and lower aromatic content of SOME contributed to earlier SOC, reducing ID in both engine configurations, especially at higher loads and CRs[54].

The combustion duration (CD) measured between CA05 (start of combustion) and CA90 (end of combustion) was generally longer for biodiesel blends compared to diesel, primarily due to their lower heating value and higher vaporization enthalpy. Despite this, increasing CR led to improved atomization and air-fuel mixing, which in turn shortened CD in both uncoated and TBC engines. In uncoated engines, the CD reduction from CR 16 to 17.5 ranged between 2.43°CA and 3.99°CA across all blends and further decreased by 2.29°CA to 5.66°CA when CR increased to 19[64]. Similarly, in TBC engines, CD was reduced further by 0.94°CA to 3.89°CA at CR 17.5 and by 0.31°CA to 3.89°CA at CR 19 compared to uncoated counterparts. These improvements in CD are attributed to the enhanced combustion environment in TBC engines, which promote higher cylinder temperature, better atomization, and faster oxidation, leading to more complete combustion. These trends were consistent with other studies involving TiO_2-coated engines running on Pongamia-based biodiesel blends[56,61].

The rate of pressure rises (RoPR), an indicator of combustion intensity and knocking tendency, increased with both engine load and CR in all test conditions. However, diesel consistently showed a higher RoPR than biodiesel blends due to its lower cetane number and longer ID, which allows for a larger fuel-air premix before ignition. In uncoated engines, the average RoPR increased by 0.2 bar/°CA when CR was raised from 16 to 17.5 and by 0.76 bar/°CA when increased to CR 19. In TBC engines, the mean RoPR increased by 0.27 bar/°CA and 0.25 bar/°CA at CR 17.5 and CR 19, respectively, compared to uncoated engines[48,67]. These results align with previous findings in engines using Karanja and roselle biodiesel blends, also demonstrated a rise in RoPR with CR. Cumulative heat release rate (CHRR), representing the total energy released during combustion, is a key metric for assessing combustion efficiency. Across all test fuels and configurations, CHRR increased with CR. Diesel consistently exhibited higher CHRR than biodiesel blends due to its higher calorific value and superior atomization characteristics. SOME blends showed comparatively lower CHRR because of their higher density, viscosity, and oxygen content, which leads to slower and more diffused combustion[58,68].

Nonetheless, TBC engines showed enhanced CHRR across all fuel blends due to increased combustion chamber temperature, better premixed zone formation, and improved oxidation. At full load in uncoated engines, CHRR increments from CR 16 to 17.5 ranged from 24.3 J to 29.98 J across blends, and from 17.08 J to 29.27 J when CR increased to 19. In TBC engines, the CHRR gains were even more notable ranging from 3.52 J to 8.55 J at CR 17.5 and from 5.78 J to 7.88 J at CR 19, depending on the blend. These enhancements confirm that thermal barrier coating, combined with higher CR, can significantly improve the combustion efficiency of biodiesel blends, narrowing the performance gap with diesel[65]. The observed trends in CHRR also correlate well with in-cylinder pressure, RoPR, and BTE values, reinforcing the mechanistic consistency of the results. Overall, this study demonstrates that biodiesel blends, particularly B20, can perform comparably to diesel in both standard and TBC engines when operated at higher CR. The application of thermal coating helps offset the limitations of biodiesel, such as lower calorific value and higher viscosity, by enhancing the combustion environment. Improved SOC, reduced ID, shorter CD, and elevated CHRR in coated engines support the viability of biodiesel as a sustainable alternative fuel, especially when paired with engine design modifications like LHR and TBC configurations[28].

Ignition lag

Ignition delay (ID) is a critical phase in compression ignition (CI) engines, representing the interval between the start of fuel injection and the onset of combustion. It is composed of both physical and chemical delay periods. The physical delay involves atomization, vaporization, air–fuel mixing, and heating of fuel droplets, while the chemical delay refers to the time required for pre-flame reactions to progress toward auto-ignition[72]. The ignition characteristics are influenced by several physico-chemical fuel properties, including cetane number, viscosity, density, latent heat of vaporization, surface tension, and in-cylinder thermodynamic conditions such as pressure and temperature. A higher cetane number typically indicates a shorter ignition delay, which is especially important in optimizing engine performance and emissions[73]. In this investigation, ignition delay was experimentally evaluated for uncoated and mullite-coated (TBC) CI engines operating under various compression ratios (CR = 16, 17.5, and 19) and engine loads using diesel and scum oil methyl ester (SOME) blends. The variation in ignition delay as a function of crank angle (CA) was plotted in Fig. 12(a–f), and supporting data is presented in Tables 5 and 6.

Across all tested fuel blends, results demonstrated that ID decreased with increasing load and compression ratio. At higher engine loads, elevated in-cylinder temperature and residual gas content promoted faster ignition due to favorable thermal conditions. Moreover, the oxygen-rich nature and higher cetane number of SOME contributed to consistently shorter ignition delay than diesel across all CRs and loads[74]. For instance, in uncoated engine at full load, the ID decreased as CR increased from 16 to 17.5 and then to 19. For B20, ID dropped from 16.24° to 15.62° CA (CR 16 to 17.5), and further to 14.82° at CR 19. Similar trends were observed for B40, B60, B80, and B100. Diesel also showed a reduction, but ID remained higher than that of SOME blends due to its lower cetane number and lack of intrinsic oxygen content. The coating of engine components with mullite further influenced ID behavior. The ceramic layer enhanced in-cylinder temperature retention, improving fuel vaporization and promoting earlier combustion. In TBC engines, ignition delay periods were significantly reduced for all fuels. At full load and CR 19, ID for B20 decreased from 15.62° (uncoated) to 13.62° CA (coated), indicating a marked improvement in ignition characteristics due to thermal insulation and improved combustion chamber conditions. This trend held true across other blends as well ID for B100 at CR 19 fell from 14.75° (uncoated) to 12.75° (coated)[75]. These observations confirm that the combination of biodiesel with ceramic-coated combustion chamber leads to faster ignition, especially at higher CRs and loads. The shortened ID facilitates an earlier start of combustion (SOC), as evident in Figs. 10 and 11, contributing to a higher peak pressure and a more efficient premixed combustion phase. This is particularly important in engine operating with SOME, where chemical reactivity is enhanced due to high oxygen availability and lower aromatic content, promoting rapid flame propagation.

The rise in compression ratio also plays a pivotal role. It leads to increased air temperature during compression, lowering the fuel auto-ignition threshold. Combined with the TBC insulating effect, this results in more favorable condition for auto-ignition. Furthermore, reduced viscosity and better atomization at high temperatures facilitate finer fuel dispersion and better mixing with air, which collectively support faster combustion initiation. The study also showed that the ignition delay is longer for diesel under all conditions due to its relatively inferior volatility, lower cetane index, and absence of internal oxygen. In contrast, SOME and its blends demonstrate consistently shorter delay periods due to better pre-flame chemistry and enhanced molecular oxygenation, especially under thermally optimized conditions provided by the TBC engine configuration[13,15]. Experimental comparisons also revealed that ID variation correlates with changes in other combustion parameters such as cylinder pressure, heat release rate (HRR), and combustion duration (CD). A shorter ID typically resulted in earlier and more intense HRR peaks, improving thermal efficiency while minimizing unburned fuel residues[58]. In summary, this investigation confirms that ignition delay is significantly influenced by fuel composition, engine coating, compression ratio, and load. The combination of biodiesel blends with ceramic-coated engine at higher CR fosters rapid ignition, enhancing combustion efficiency. The synergy between fuel properties and engine design parameters offers a viable path for cleaner and more efficient CI engine operation, with particular promise for sustainable biodiesel application.

Emission characteristics

According to theory, the ideal combustion of the fuel-air mixture in the diesel engine cylinder would result in the formation of just CO_2 and water (H_2O), as shown in Eq. 8. Nevertheless, attaining full combustion in real-world situations is difficult due to a range of engine operating factors. The parameters encompassed in this set are the fuel-air equivalency ratio, fuel type, combustion chamber design, oxygen availability, autoignition temperature of the fuel, ignition lag, and fuel vaporization ratio. Fluctuations in various operational parameters lead to energy wastage from the fuel provided. Equation 9 shows that when fuel undergoes incomplete combustion, it produces damaging pollutants including CO, CO_2, NO_x, HC, and other substances.

$$C_xH_y + z(O_2) \rightarrow a\,(CO_2) + b\,(H_2O) + Energy \tag{8}$$

where, x = a, y = 2b and z = 2a + b.

$$C_xH_y + z(O_2) \rightarrow a\,(CO_2) + b\,(H_2O) + c\,(CO) + d\,(HC) + e\,(PM) + Energy \tag{9}$$

Emission like CO and HC in the exhaust is very important because which indicates that fuel is not completely utilized such that less chemical energy obtained from the fuel[76]. Emissions such as CO_2 and NO_x emitted by CI engine will greatly affect the ozone layer and on human health. The diesel engine emission in with and without coated engine with diesel and SOME blends were evaluated in terms of CO, CO_2, O_2, NO_x, HC and smoke opacity at various CRs (16,17.5 and 19) and at various loading conditions of the engine.

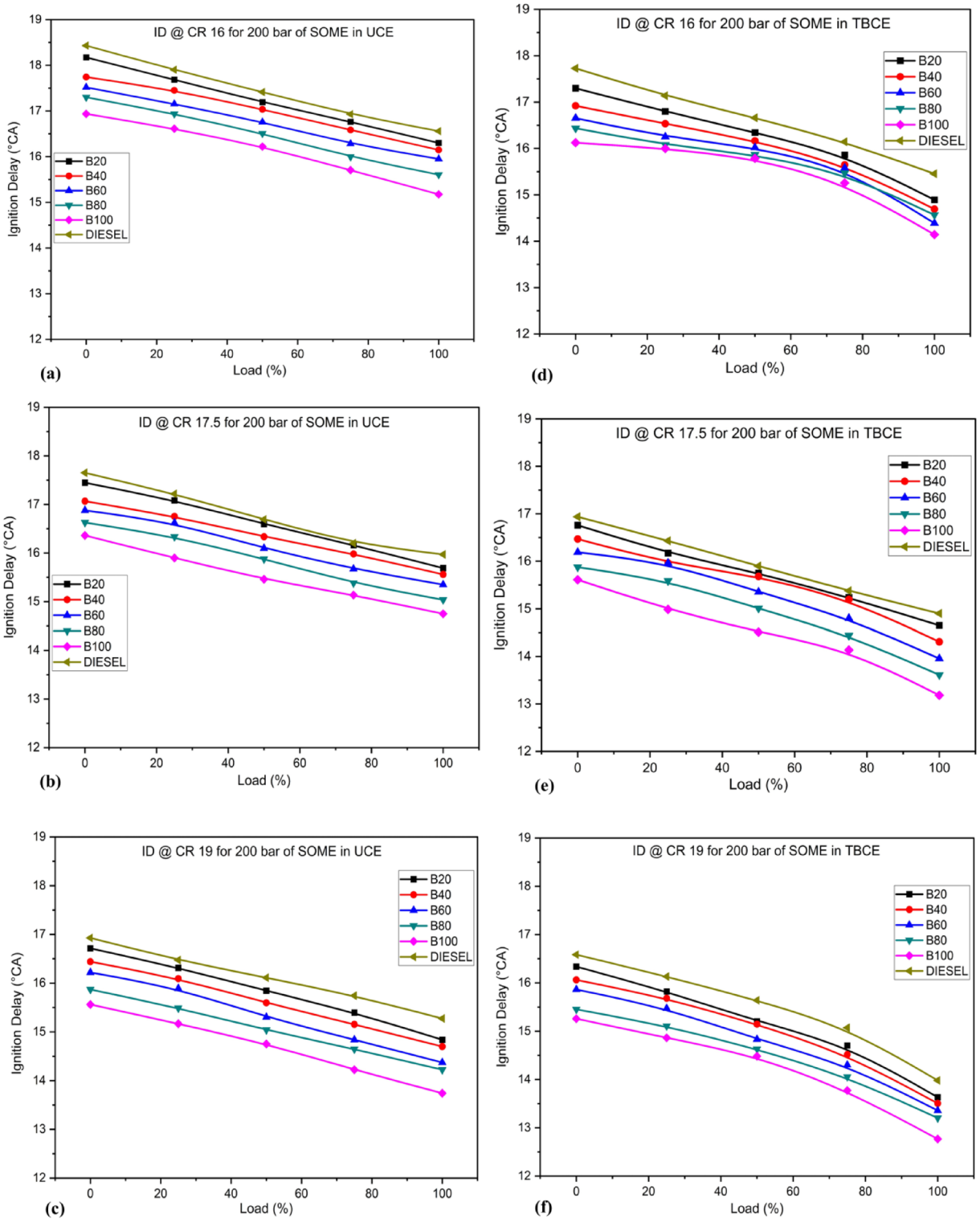

Fig. 12. (**a**–**f**) The fluctuations in ID at various loads and CRs (16, 17.5, & 19) for blends of SOME in both coated and uncoated engines.

Carbon monoxide (CO)

Carbon monoxide (CO) emissions in CI engines arise primarily from incomplete combustion, often due to insufficient oxygen availability, poor fuel–air mixing, suboptimal injection timing, low injection pressure, and engine design limitations. CO is a harmful, odorless, and colorless gas that must be strictly minimized. Experimental results presented in Fig. 13(a–f) show that CO emissions were consistently lower for all SOME blends compared to diesel across various compression ratios (CRs) in both uncoated and thermal barrier-

CR	Fuel Type	SOI °CA	SOC °CA	EOC °CA	ID °CA	CD °CA	CCP_{max} bar	θCCP_{max} °CA	R_{max} bar/°CA	θR_{max} °CA	MGT_{max} °C	θMGT_{max} °CA	HRR_{max} J/°CA	θHRR_{max} °CA	$CHRR_{max}$ J	$\theta CHRR_{max}$ °CA
16	B20	−25.18	−8.94	40.5	16.24	49.44	65.03	9	3.825	−3	1464.95	25	39.98	−2	1064.23	86
	B40	−25.7	−9.39	41.5	16.31	50.89	64.54	10	3.692	−3	1453.87	25	37.37	−3	1052.25	87
	B60	−25.7	−9.75	43.5	15.95	53.25	63.68	9	3.682	−3	1443.28	25	36.25	−2	1051.65	86
	B80	−25.46	−9.85	45	15.61	54.85	64.08	9	3.625	−3	1432.09	25	34.39	−2	1048.88	85
	B100	−25.03	−9.85	46.5	15.18	56.35	63.69	10	3.399	−4	1423.26	24	33.74	−4	1036.62	86
	DIESEL	−26.74	−10.19	39	16.55	49.19	65.84	10	4.894	−4	1470.92	25	42.3	−4	1071.68	89
17.5	B20	−23.06	−7.44	39	15.62	46.44	72.36	9	4.23	−5	1474.12	23	46.97	−1	1091.45	92
	B40	−23.83	−8.28	40	15.55	48.28	71.26	9	3.918	−4	1463.93	22	44.78	−1	1082.23	90
	B60	−23.91	−8.57	41.5	15.34	50.07	70.76	9	3.799	−4	1452.24	22	43.12	−1	1075.95	91
	B80	−24.44	−9.42	43	15.02	52.42	69.96	9	3.646	−3	1444.54	22	39.87	−2	1077.67	91
	B100	−23.61	−8.86	44	14.75	52.86	69.33	9	3.539	−4	1432.98	23	36.34	−2	1061.21	93
	DIESEL	−23.66	−7.7	37.5	15.96	45.2	73.46	8	4.93	−5	1478.77	22	47.49	−1	1099.35	92
19	B20	−23.49	−8.67	35	14.82	43.67	73.67	7	4.894	−6	1481.15	21	45.82	−1	1118.85	94
	B40	−23.24	−8.46	35.5	14.78	43.96	72.83	7	4.889	−6	1470.12	21	44.12	−2	1101.16	94
	B60	−22.77	−8.41	36	14.36	44.41	72.29	7	4.695	−6	1460.17	20	41.85	−3	1096.45	93
	B80	−22.83	−8.61	38.5	14.22	47.11	71.95	8	4.655	−6	1449.06	21	41.79	−2	1094.75	92
	B100	−24.31	−10.57	40	13.74	50.57	70.85	7	4.358	−5	1438.88	21	41.23	−4	1079.92	90
	DIESEL	−22.63	−7.35	34	15.28	41.35	74.38	8	5.135	−7	1489.35	20	47.97	−1	1128.62	95

Table 5. Combustion and fuel injection characteristics of UCE for different fuel samples and CR at peak engine load.

coated (TBC) engines. At light and medium loads, SOME blends produced noticeably lower CO levels. However, under peak load, CO emissions rose due to richer mixtures and reduced combustion duration. The additional oxygen content in SOME improves oxidation reactions, leading to cleaner combustion. Increasing the biodiesel proportion in the blend further lowered CO emissions, confirming the emission-reducing potential of oxygenated fuels like SOME in LHR and standard CI engines[77]. Furthermore, under steady-state engine operating conditions, the oxygen content of biodiesel increases the oxidation of CO to CO_2, as demonstrated by Eqs. 10 and 11. Despite higher BSFC, biodiesel blends exhibit lower CO emissions due to their inherent oxygen content, higher cetane number, and improved combustion phasing, which collectively enhance oxidation efficiency. Additionally, elevated in-cylinder temperatures in LHR engines accelerate CO-to-CO_2 conversion, further reducing CO emissions even under rich or high-load conditions[78].

$$x\,(CO) + Y(O_2) \rightarrow (CO_2) + Energy \tag{10}$$

where, $y = \frac{x}{2}$

$$C + O_2 \rightarrow CO_2 + Energy \tag{11}$$

Blends of biodiesel contain higher cetane number, which lowers the probability of fuel rich-zones formation and with advanced injection and combustion when using biodiesel justify the reduction of CO emission[37,38]. As scrutinized from the Fig. 13(a – f) showed reduced CO emission for all tested samples at increasing CR from 16:1 to 19:1 at maximum load in with and without coated engine. When the CR increased from 16 to 17.5, the CO emission decreased by 9.09%, 15.79%, 25%, 13.33%, 17.14%, and 7.41% for the blends of B20, B40, B60, B80, B100, and diesel respectively at full load for an uncoated engine. Similarly, when the CR is increased from 17.5 to 19, the CO emission decreased by 10%, 11.76%, 6.67%, 25%, 40%, and 12.5% for the same blends. The likely cause for this pattern is the rise in CR and engine load while maintaining the same injection time, resulting in elevated cylinder pressure and air temperature within the cylinder. Which improves atomization for a large amount of fuel and consequently reduces the ignition day period causing improved combustion process which results in reduced CO emission at higher CR. Hirkude et al.[79] and Sivaramakrishnan[78] reported that CO emission level decrease with increasing biodiesel percentage and compression ratio. As shown in Fig. 13(d–f), mullite-coated diesel engines had greater combustion efficiency for all fuels, reducing CO emissions. Average CO emission reduce in the coated engine was determined to be 10%, 11.76%, 6.67%, 15.38%, 16.67% and 8% at CR-17.5 and 5.26%, 6.25%, 7.14%, 9.09%, 3.09% and 9.09% at CR-19 for B20, B40, B60, B80, B100 and diesel respectively at peak load when compared to uncoated engine. In this study, carbon monoxide (CO) emissions decreased significantly by up to 40% for SOME blends and 12.5% for diesel when the compression ratio increased from 17.5 to 19. Overall, a 20–50% reduction in CO emissions was observed in the Low Heat Rejection (LHR) engine as compression ratio rose from 16 to 19, as shown in Figure S-8. This trend is similar to the results found by Ramasamy et al., where Y_2O_3–ZrO_2 and Al_2O_3–SiO_2 coatings on palm biodiesel-fueled engines effectively lowered CO levels[80]. The decline in CO emissions is primarily attributed to enhanced in-cylinder heat retention from the mullite-based thermal barrier coating (TBC), improved combustion due to higher wall temperatures, and the inherent oxygen content in SOME, all of which promote more complete combustion and reduced heat loss to the coolant and ambient surroundings.

Hydrocarbon (HC) emission

Hydrocarbons (HCs) are mainly caused by incomplete combustion of petroleum diesel fuels, and are typically quantified as parts per million (ppm) of carbon atoms. These hydrocarbons are regarded as exhaust gases and are a matter of environmental concern. Major sources of HC emissions are unburnt fuel-air mixtures, HC emissions bleeding out from engine lubricating oil as well as suboptimal mixing and combustion. The chemical composition of the fuel plays a crucial role in the magnitude of these emissions fuels rich in aromatics and olefins typically produce more reactive hydrocarbon species. Variation of unburned hydrocarbon (UHC) emissions with compression ratio (CR) and engine load is illustrated in Figure 14 (a–f) for mullite-coated (TBC) and uncoated engines operated with SOME-diesel blends. At all test operating modes, SOME blends had lower HC emissions compared to neat diesel. The decrease was likely due to the higher oxygen content (10–13 wt%) in SOME, which leads to an improved combustion of the fuel and its higher cetane number, which shortens ignition delay. Such properties enhance complete combustion and the consequent reduction of fuel-rich and over-lean areas leading to higher HC emissions[81].

Typically, HC emissions are a significant problem at very high loads in diesel engines. At high loads, a larger amount of fuel is injected onto the cylinder surface, causing improper fuel distribution with less surplus air and higher wall temperatures, leading to regions where the fuel-air mixture may survive and escape into the exhaust manifold as HC emissions. This study's results indicate that HC emissions decrease with an increase in compression ratio for all tested fuels in both LHR and uncoated engines[82]. Hydrocarbon emissions for B20, B40, B60, B80, and B100 decreased by 14%, 18.75%, 18.75%, 12.28%, and 26.67% at CR-17.5 and by 4.44%, 9.3%, 17.5%, 30.55%, and 42.42% at CR-19 compared to diesel in an uncoated engine at full load. Similar results were obtained at a compression ratio of 16. The probable reason for the decrease in HC emissions at higher CRs is that biodiesel blends reach ignition temperature due to the higher wall temperature and pressure inside the engine cylinder, enabling the oxidation reaction with more O_2 molecules, which promotes complete combustion. The reductions in hydrocarbon emissions at 100% load when the CR varied from 16 to 17.5 were 20%, 12.5%, 4.17%, 4.26%, 0%, and 19.29%, and when the CR varied from 17.5 to 19, the reductions were 11.11%, 11.63%, 20%, 30.56%, and 21.28% for B20, B40, B60, B80, B100, and diesel, respectively, in an uncoated engine.

CR	Fuel Type	SOI °CA	SOC °CA	EOC °CA	ID °CA	CD °CA	CCP_{max} bar	θCCP_{max} °CA	R_{max} bar/°CA	θR_{max} °CA	MGT_{max} °C	θMGT_{max} °CA	HRR_{max} J/°CA	θHRR_{max} °CA	$CHRR_{max}$ J	$\theta CHRR_{max}$ °CA
16	B20	−24.88	−10	38	14.88	48	71.79	9	4.11	−3	1472.4	24	42.78	−2	1072.7	88
	B40	−23.64	−8.97	39.5	14.67	48.47	70.75	8	3.868	−3	1460.65	25	39.98	−2	1062	87
	B60	−23.8	−9.42	41	14.38	50.42	70.22	8	3.769	−3	1449.83	25	37.37	−3	1060.4	87
	B80	−24.35	−9.79	42.5	14.56	52.29	69.41	8	3.745	−3	1438.54	25	36.25	−2	1058.4	85
	B100	−24	−9.86	44.5	14.14	54.36	68.65	9	3.519	−4	1429.04	25	34.39	−2	1045.4	87
	DIESEL	−23.7	−8.26	37	15.44	45.26	73.01	8	4.975	−4	1478.8	24	45.60	−2	1080.2	90
17.5	B20	−22.36	−7.72	37	14.64	44.72	73.47	8	4.36	−5	1480.87	22	46.60	−1	1098.2	94
	B40	−21.7	−7.39	38.5	14.31	45.89	72.14	9	4.228	−4	1470.4	23	45.97	−1	1088.7	92
	B60	−22.24	−8.29	40	13.95	48.29	71.26	9	4.039	−4	1458.58	22	44.78	−1	1082.29	91
	B80	−22.18	−8.57	41	13.61	49.57	70.76	9	4.035	−3	1448.06	22	43.12	−1	1081.19	91
	B100	−22.6	−9.42	42.5	13.18	51.92	69.48	10	3.789	−4	1437.82	23	39.87	−2	1066.05	93
	DIESEL	−22.32	−7.44	36	14.88	43.44	74.78	8	5.225	−5	1487.32	22	47.97	−1	1107.9	93
19	B20	−22.04	−8.42	34	13.62	42.42	74.94	6	5.124	−6	1489.62	20	47.97	−1	1126.3	95
	B40	−22.28	−8.78	34.5	13.5	43.28	73.88	6	5.099	−6	1479.87	20	45.82	−1	1107.94	94
	B60	−21.86	−8.52	35.5	13.34	44.02	72.75	6	4.935	−6	1468.92	21	44.12	−2	1103	94
	B80	−21.68	−8.48	37	13.2	45.48	72.29	7	4.925	−6	1458.58	21	41.85	−3	1101.2	93
	B100	−21.43	−8.68	38	12.75	46.68	71.95	8	4.608	−5	1447.66	22	41.79	−2	1085.7	92
	DIESEL	−22.62	−8.66	33	13.96	41.66	76.58	6	5.445	−7	1497.87	20	49.62	−1	1136.5	97

Table 6. Combustion and fuel injection characteristics of TBCE for different fuel samples and CR at peak engine load. CPmax: Maximum Combustion In-Cylinder Pressure, θCCPmax: Angle of Maximum Combustion In-Cylinder Pressure, Rmax: Maximum Pressure Rise Rate, θRmax: Angle of Maximum Pressure Rise Rate, MGTmax: Maximum Mean Gas Temperature, θMGTmax: Angle of Maximum Mean Gas Temperature, HRRmax: Maximum Heat Release Rate, θHRRmax: Angle of Maximum Heat Release Rate.

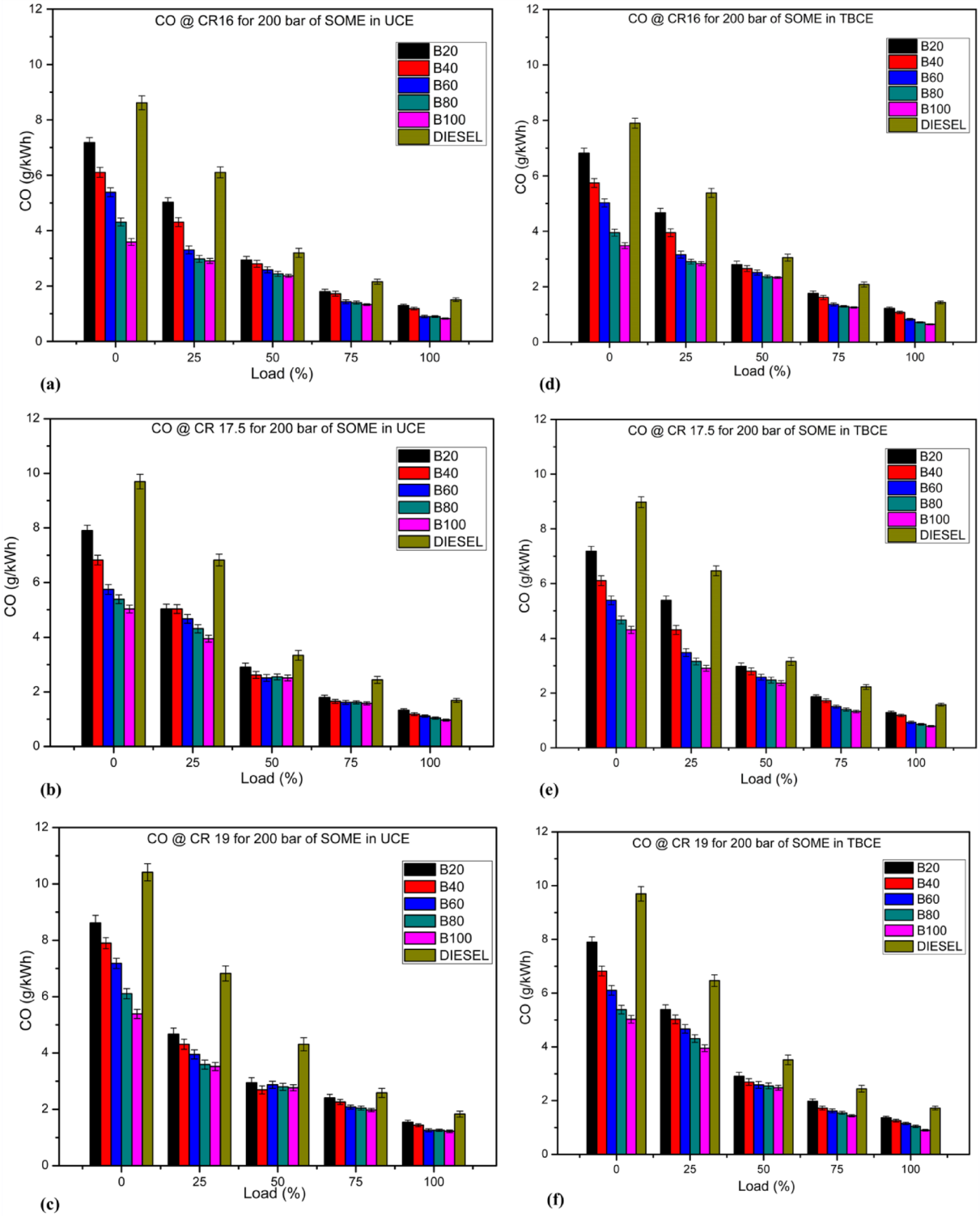

Fig. 13. (**a**–**f**). The variation of the CO at different loads and CRs (16, 17.5 & 19) for SOME blends in both coated and uncoated engines.

Results show that HC emissions are lower in the TBC engine compared to the uncoated engine for all test fuels at maximum load and different CRs, as demonstrated in Figure S-9. Hydrocarbon emissions from the mullite-coated engine decrease significantly compared to the uncoated engine due to the shorter quenching distance, increased after-combustion temperature, and lower flammability limit associated with the TBC engine, resulting in reduced heat loss to the cooling system. By harnessing thermal energy within the combustion chamber, the combustion of the fuel-air mixture is enhanced, leading to decreased HC emissions[83]. The reductions in HC

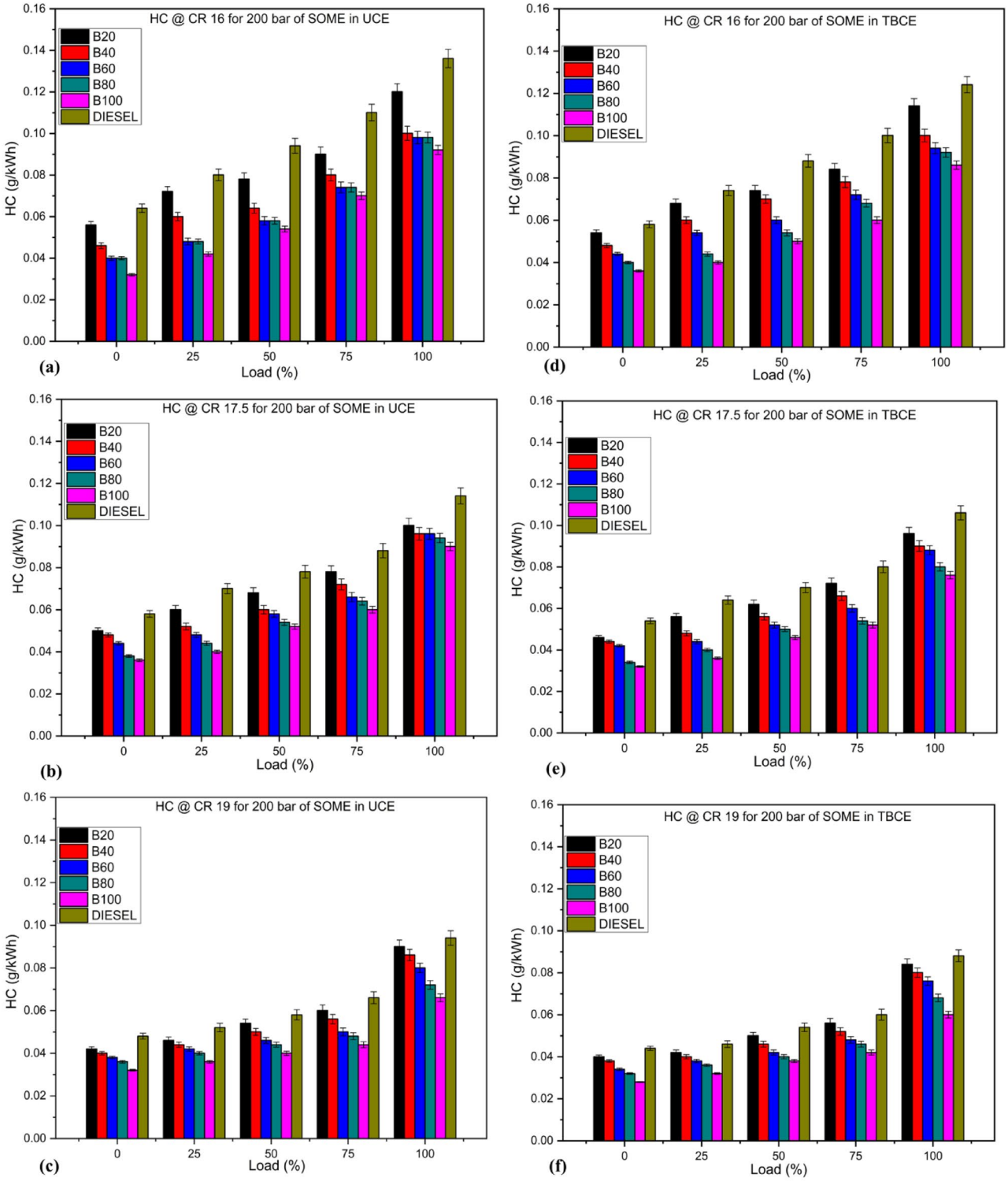

Fig. 14. (**a**–**f**). The variation of the HC at different loads and CRs (16, 17.5 & 19) for SOME blends in both coated and uncoated engines.

emissions at full load in the LHR engine are 4.17%, 6.67%, 9.09%, 17.5%, 18.42%, and 7.55% at CR-17.5 and 7.14%, 7.55%, 5.26%, 5.88%, 10%, and 6.82% at CR-19 for B20, B40, B60, B80, B100, and diesel, respectively, compared to the standard diesel engine. In the present study, HC emissions were reduced by 42.42% for B100 and 26.67% for B20 with increased CR from 17.5 to 19, with overall reductions ranging from 12 to 42% in the uncoated engine and 5–18% in the LHR engine. These results are in close agreement with previous studies, including 39.1% with Orange Peel biodiesel in TBC engine[69,80]. The improved performance in the mullite-coated

engine is primarily due to higher in-cylinder and gas temperatures, which promote efficient oxidation. This results in a more complete combustion, especially on oxygen rich SOME blends, leading to lower unburned hydrocarbon emissions.

Nitrogen oxide (NO_x) emission

Nitrogen oxides (NO_x) have been and continue to be one of the most challenging and complex emissions faced by biodiesel and its blends in compression ignition (CI) engines. NO_x is generated mostly by thermal oxidation of atmospheric nitrogen, promoted at high in-cylinder temperatures (usually above 1500 K), high oxygen levels and long combustion times. These conditions facilitate the Zeldovich mechanism, the dominant pathway for NO_x formation[84]. The oxygen content, cetane number of biodiesels, and its properties such as density, viscosity, and compressibility have a considerable effect on fuel atomization, injection pressure, and combustion characteristics, leading to NO_x emission. Figure 15(a-f) depicts the influence of engine load on NO_x emission for different SOME-diesel fractions at different compression ratios (CRs) for uncoated and TBC engines. NO_x emissions had a tendency to increase with increased CRs and increasing biodiesel contents, as a result of the higher combustion temperature and more complete fuel oxidation. Also, the decreased soot generation with biodiesel, known as combustion heat absorber, increases flame temperature for NO_x formation. The contribution to higher adiabatic flame temperatures is due also to the existence of unsaturated bonds in SOME. In general, although combustion efficiency is enhanced due to biodiesel oxygenated composition of fuel and its thermal behavior, NO_x abatement becomes a major issue with the use of oxygen-based biodiesel especially under high CRs[85,86].

For uncoated engines, NO_x emissions for B20, B40, B60, B80, B100, and diesel increased on average by 21.38%, 22.49%, 23.33%, 22.27%, 14.97%, and 20.27%, respectively, when the CR was increased from 16 to 17.5. With a further increase in CR from 17.5 to 19, the corresponding values were 6.21%, 5.49%, 4.72%, 4.15%, 4.41%, and 6.77%, respectively. This indicates that higher CR benefit biodiesel more than conventional diesel, due to its volatility, higher viscosity, density, and cetane number, which enhance performance at higher CRs. Diesel and SOME blends exhibit higher NO_x emissions in LHR engines at all CRs compared to uncoated engines, as shown in Fig. 15(d–f). The increased NO_x formation in TBC engines is due to higher post-combustion temperatures and longer combustion periods, causing an earlier SOC and shifting the peak temperature and pressure closer to TDC[64]. Consequently, most of the fuel burns in the premixed stage, leading to increased NO_x formation. Even in coated engines, NO_x emissions for SOME blends are higher than for diesel fuel due to the higher oxygen content in vegetable oils and traces of nitrogen in biodiesel[78]. NO_x emissions for B20, B40, B60, B80, B100, and diesel were found to be 827, 840, 855, 855, 871, 894, and 814 ppm at CR-17.5, and 838, 852, 868, 882, 915, and 826 ppm at CR-19, respectively, for mullite-coated engines at higher load. This shows that for coated engines, NO_x emissions increased by 1.59%, 1.45%, 1.78%, 1.87%, 2.76%, and 2.26% at CR-17.5, and by 2.07%, 2.16%, 2.12%, 2.2%, 3.16%, and 1.97% at CR-19 compared to uncoated engines. Finally, SOME and its blends used in both LHR, and standard diesel engines result in higher NO_x formation compared to diesel, as shown in Figure S-10, consistent with findings from various studies. To mitigate NO_x emissions without compromising engine performance, strategies such as Exhaust Gas Recirculation (EGR), injection timing retardation, split injection, and water or steam injection can effectively lower peak combustion temperatures. In thermal barrier-coated engines, where in-cylinder heat retention is higher, post-combustion control technologies like Selective Catalytic Reduction (SCR) and Lean NO_x Traps (LNTs) become essential for achieving further NO_x reduction[87].

Smoke opacity

Smoke opacity is significant because it gives indication of the concentration of pollutants due to soot particle formation with the dearth of oxygen content and their oxidation rate even in the presence of some hydrocarbon, paying way for higher smoke emission which leaves smokestack. Higher smoke emission is generated when fossil fuels are burnt in the diesel engine due to extreme air deficiency. In CI engine, the main combustion of fuel occurs via diffusion mechanism during which the atomized fuel particles are broken down into two primary elements as carbon (soot formation) that will be oxidized in the reaction zone (soot oxidation)[88]. If there is deficiency of oxygen content and if combustion temperature does not support the oxidation process, smoke (carbonaceous particle) will be released in the exhaust gaseous. Fuels with higher viscosity tend to increase smoke emissions due to a lower air-fuel mixing rate and larger mean fuel spray droplet size. Smoke emission from diesel engines results from incomplete combustion, which can lead to higher fuel consumption and oil loss at elevated temperatures. Figure 16(a–f) illustrates the relationship between smoke opacity emissions and load for all tested fuels (SOME) at various CRs in both uncoated and coated engines. Using biodiesel blends, there is a significant reduction in smoke output in both LHR and uncoated engines when the CR rises from 16 to 19, irrespective of load level. Fuel consumption decreases due to better combustion efficiency and more oxygen-rich molecules, which enable more complete combustion. The decrease in smoke emission with higher biofuel percentages is due to the reduced carbon content in blended fuels, which have fewer C-C bonds compared to diesel, leading to lower smoke opacity. The impact of biodiesel addition on smoke emission is more significant at higher loads because the premixed combustion fraction decreases as the diffusion CD increases[87]. At maximum load, for every 20% increase in biodiesel blending in diesel, the smoke opacity reduction at CR-17.5 is 8.09%, 13.64%, 12.74%, 17.17%, and 24.76%, and the corresponding values at CR-19 are 5.27%, 9.91%, 15.19%, 17.45%, and 24.79% lower than standard diesel. Figure S-11 shows that at peak load, smoke opacity is lower at higher CRs compared to lower ones. This is because higher CRs increase the operating temperature and pressure, enhancing combustion efficiency. Improved reaction between fuel and air reduces smoke emissions in both coated and uncoated engines. Smoke emissions in the LHR engine decreased by 5.94%, 5.37%, 12.82%, 12.45%, 11.23%, and 8.8% at CR-17.5 and by 6.95%, 5.62%, 7.66%, 12.33%, 12.41%, and 8.12% at CR-19 for B20, B40, B60, B80, B100, and diesel, respectively, compared to the uncoated engine. These values show that all biodiesel blends in the

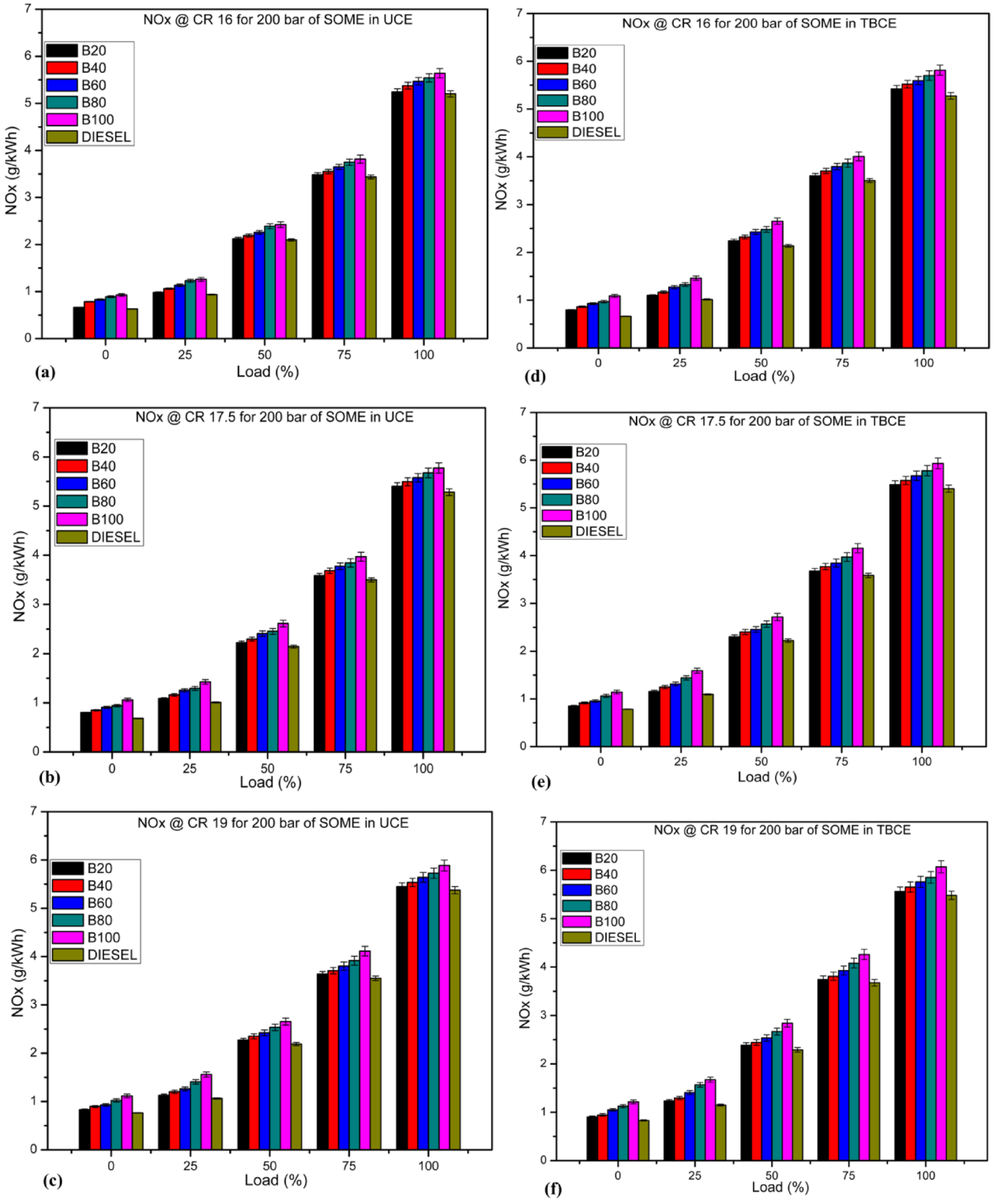

Fig. 15. (**a**–**f**) The variation of the NO_x at different loads and CRs (16, 17.5 & 19) for SOME blends in both coated and uncoated engines.

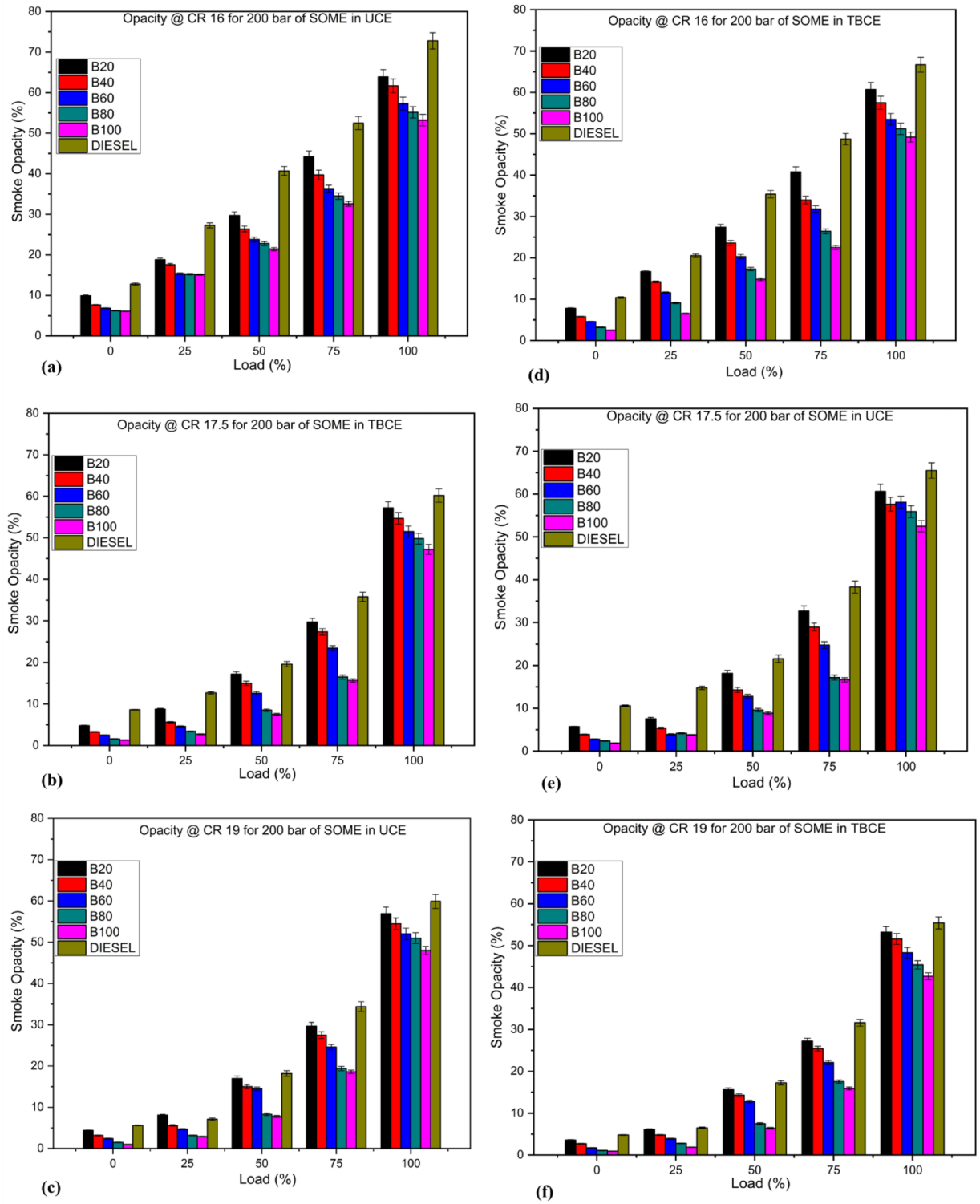

Fig. 16. (**a**–**f**). The variation of the smoke opacity at different loads and CRs (16, 17.5 & 19) for SOME blends in both coated and uncoated engines.

coated engine reduce smoke opacity, despite SOME's higher viscosity and molecular weight. The excess heat in the TBC engine raises combustion chamber temperature, oxidizing soot and promotes complete combustion due to abundant oxygen, minimizing smoke emissions. These findings align with other studies in the literature[4,29].

Carbon dioxide (CO_2)

CO_2 emissions in CI engines result from the thorough burning of traditional fuels, functioning as a measure of combustion effectiveness. CO_2 is a significant greenhouse gas contributing to global warming. Higher CO_2 concentrations in the exhaust indicate improved combustion efficiency, contrasting with CO emissions. Factors influencing CO_2 emissions include viscosity, density, combustion chamber design, air-fuel equivalence ratio, SOI, fuel line pressure, and engine speed. The CO_2 emissions from biodiesel combustion are less impactful on the atmosphere since they are primarily absorbed by plants, trees, and crops. The simultaneous reduction in CO and CO_2 emissions for biodiesel blends is attributed to their inherent oxygen content, which promotes complete combustion with lower carbon intensity per unit energy. Despite improved oxidation, the overall CO_2 output remains lower due to biodiesel's lower carbon content and biogenic origin, resulting in a reduced net greenhouse gas impact[29].

Figure 17(a–f) presents the results of CO_2 emissions for different engine loads and CRs in both uncoated and coated engines using blends of SOME and diesel fuel. The data shows that CO_2 concentrations rise with increasing load and CRs for all test fuels in both engine types. Additionally, CO_2 emissions decrease with higher proportions of SOME blends compared to diesel fuel. Several studies have demonstrated a decrease in CO_2 emissions while utilizing biodiesel blends in diesel engines. This reduction can be due to the presence of 10–12% excess oxygen molecules in biodiesel. The highest CO_2 emission values for diesel were 10.12% at CR-17.5 and 10.57% at CR-19, while for B20, B40, B60, B80, and B100 at CR-17.5, the values were 9.95%, 9.7%, 9.22%, 9.07%, and 8.93%, respectively. At CR-19, the values were 10.21%, 9.63%, 9.42%, 9.11%, and 8.92%, respectively, all lower than those for diesel at full load in an uncoated engine. The increase in CO_2 emissions with load is due to the higher amount of fuel injected, leading to increased combustion temperature and oxidation rates. Higher CRs elevate post-combustion temperatures and, with sufficient oxygen in the engine chamber, enhance CO_2 emissions, indicating efficient burning[5].

Engines with mullite coating show further increases in CO_2 emissions for all samples at rated engine load. CO_2 formation in LHR engines at operating load is 10.24%, 9.88%, 9.48%, 9.21%, 8.96%, and 10.64% at CR-17.5 and 10.43%, 10.12%, 9.74%, 9.55%, 9.15%, and 10.97% at CR-19 for B20, B40, B60, B80, B100, and diesel, respectively, as shown in Fig. 18(d–f). There is a slight increase in CO_2 emissions in LHR engines, with values of 2.91%, 1.85%, 2.82%, 1.54%, 0.33%, and 5.14% at CR-17.5 and 2.15%, 5.08%, 3.39%, 4.83%, 2.57%, and 3.78% at CR-19, respectively, compared to uncoated engines, as depicted in Figure S-12. Various studies have shown that using biodiesel can reduce global greenhouse gas emissions, leading to a 50–80% decrease in CO_2 emissions compared to fossil fuels[9].

Table S-6 in the supplemental paper details the experimental results for performance, combustion, and exhaust gas emission parameters of mullite-coated CI engines at CR 19 for all fuel samples (B20, B40, B60, B80, B100, and Diesel). The comparison is conducted at peak load, ranking the results from highest to lowest. Figure S-13 illustrates the average percentage differences in performance, combustion, and exhaust emission parameters for the test samples B20, B40, B60, B80, and B100 at maximum load compared to conventional diesel fuel (D100). This comparison applies to both coated and uncoated CI engines at CR 17.5 and 19.

Conclusion

In this experimental study, scum oil methyl ester (SOME) was blended with diesel in varying proportions (B20, B40, B60, B80, B100) and tested against neat diesel (D100) in a single-cylinder VCR diesel engine, with and without a 500 µm mullite thermal barrier coating on the piston crown, cylinder head, and valves. The effects of compression ratio (CR 16:1, 17.5:1, and 19:1) on engine performance, combustion, and emissions were thoroughly evaluated.

1. The results demonstrated that increasing CR enhanced brake thermal efficiency (BTE) and reduced brake specific fuel consumption (BSFC) and brake specific energy consumption (BSEC) for all fuels. Notably, at CR 19, the coated engine achieved a 4.43% increase in BTE, a 7.98% reduction in BSFC, and an 8.19% reduction in BSEC compared to the uncoated engine, primarily due to improved thermal retention and combustion kinetics.
2. The coated engine exhibited higher exhaust gas temperatures and earlier peak cylinder pressures, indicating enhanced heat utilization. Ignition delay (ID) was consistently lower in the coated engine owing to higher in-cylinder temperatures, improved vaporization, and reduced ignition lag.
3. Advancements in start of injection (SOI) timing were observed with increasing CR, with SOI deviations reducing from −0.751°CA at CR 17.5 to −0.212°CA at CR 19 in the uncoated engine. Diesel showed shorter combustion duration (CD) and higher cumulative heat release rate (CHRR) than SOME blends due to better atomization and higher heating value, while SOME exhibited smoother but slower combustion, attributed to its high viscosity, density, and oxygen content.
4. Emission analysis revealed a consistent decrease in CO, HC, and smoke opacity with higher biodiesel blend ratios and CRs, attributed to the oxygenated nature of biodiesel promoting more complete combustion. Compared to the uncoated engine, the coated engine at CR 17.5 and 19 achieved average reductions in CO by 11.41% and 6.65%, HC by 10.56% and 7.10%, and smoke opacity by 9.43% and 8.84%, respectively.
5. NO_x emission increased due to higher flame temperature and oxygen content, with coated engine showing average NO_x increase of 4.56% at CR 17.5 and 1.39% at CR 19. CO_2 emission slightly increased in the coated engine due to more complete oxidation, with average rises of 2.43% and 3.63% at CR 17.5 and CR 19, respec-

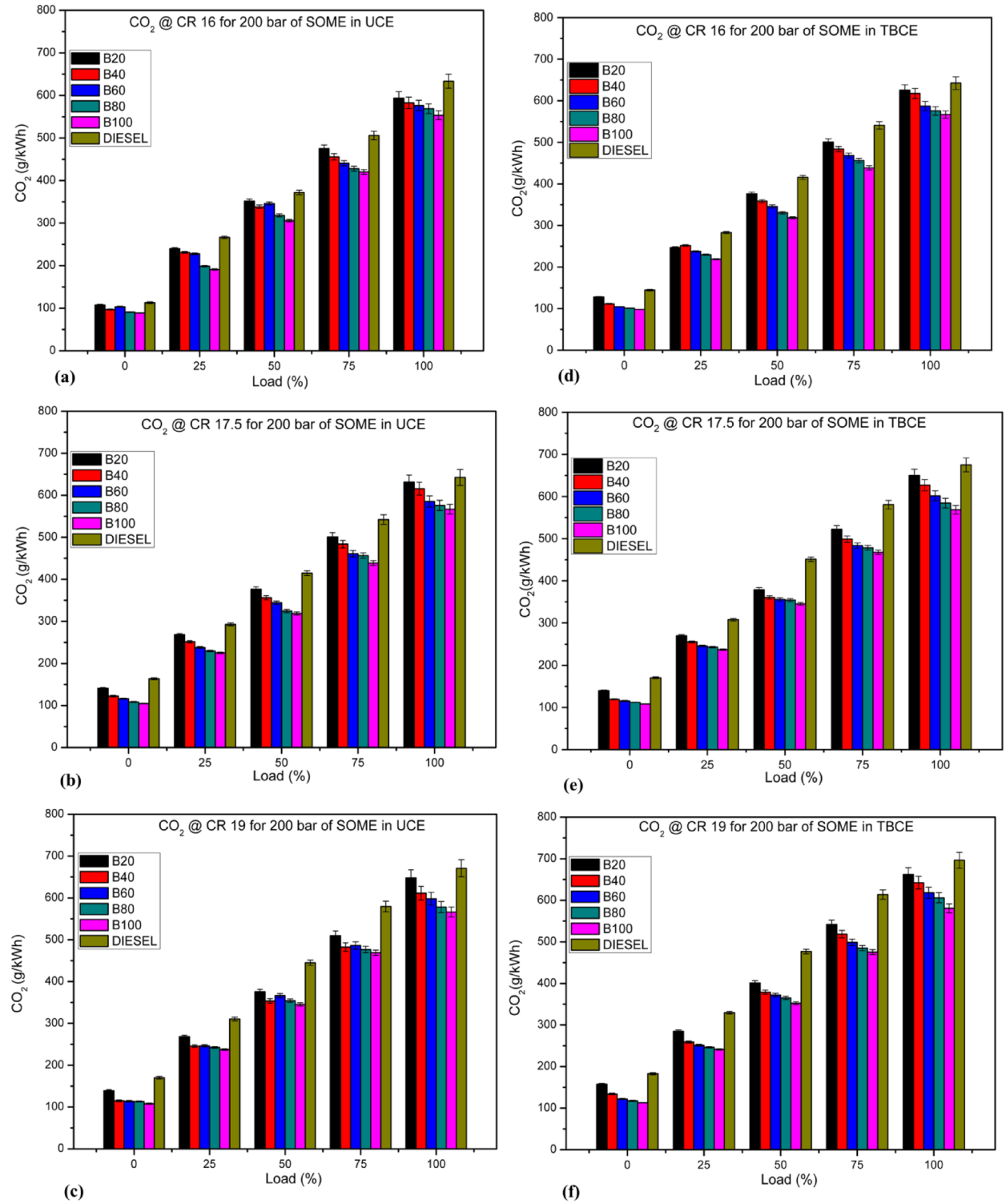

Fig. 17. (**a**–**f**). The variation of the CO_2 at different loads and CRs (16, 17.5 & 19) for SOME blends in both coated and uncoated engine.

tively, though overall CO_2 levels remained lower for higher SOME blends compared to diesel due to their lower carbon content.

6. Among all test fuels, the B20 blend exhibited optimal performance, combustion behavior, and emission profile, particularly in the coated engine at CR 19, making it a promising candidate for diesel replacement.

7. Furthermore, utilizing waste-derived scum oil for biodiesel production offers notable economic and environmental benefits, including reduced fossil fuel dependency, lower carbon emission, and sustainable waste valorization.

Future Work

Future research should explore advanced exergy, exergoeconomic, and enviroeconomic analyses to optimize system performance holistically. Additionally, integrating in-cylinder NO_x mitigation strategies such as EGR, injection timing optimization, split injection, and water or steam injection along with post-combustion control technologies like SCR and LNTs will be essential, particularly for thermal barrier-coated engines, to achieve cleaner and more efficient combustion. Additionally, prospective studies will investigate mullite coating durability through thermal fatigue testing and microstructural analysis to evaluate long-term performance under cyclic engine operating conditions.

Data availability

The data that supports the findings of this study are available within the article.

Received: 21 June 2025; Accepted: 1 August 2025
Published online: 24 August 2025

References

1. Sakthivel, R., Ramesh, K., Purnachandran, R. & Mohamed Shameer, P. A review on the properties, performance and emission aspects of the third generation biodiesels. *Renew. Sustain. Energy Rev.* **82**, 2970–2992. https://doi.org/10.1016/j.rser.2017.10.037 (2018).
2. Suresh, M., Jawahar, C. P. & Richard, A. A review on biodiesel production, combustion, performance, and emission characteristics of non-edible oils in variable compression ratio diesel engine using biodiesel and its blends. *Renew. Sustain. Energy Rev.* **92**, 38–49. https://doi.org/10.1016/j.rser.2018.04.048 (2018).
3. Erdi Gülcan, H., Bayindirli, C., Erol, D. & Çelik, M. Role of different type nanoparticles on exergy, thermoeconomic, exergoeconomic, environmental, and enviroeconomic indicators in a CI engine fueled with rapeseed oil biodiesel. *Fuel* **384**, 134074. https://doi.org/10.1016/j.fuel.2024.134074 (2025).
4. Jain, A. et al. Deden ramdan, and Muhammad Imam ammarullah. Strategies for enhanced management of cleaner diesel combustion with nanoparticle additives: A critical review with biomedical considerations. *Ain Shams Eng. J.* **15** (12), 103118. https://doi.org/10.1016/j.asej.2024.103118 (2024).
5. Magesh, N. et al. Experimental Investigation and Prediction of Performance, Combustion, and Emission Features of a Diesel Engine Fuelled with Pumpkin-Maize Biodiesel using Different Machine Learning Algorithms. *Mathematical Problems in Engineering* no. 1 (2022): 9505424. (2022). https://doi.org/10.1155/2022/9505424
6. Aljaafari, A. et al. Biodiesel emissions: A State-of-the-Art review on health and environmental impacts. *Energies (Basel)*. **15**, 6854. https://doi.org/10.3390/en15186854 (2022).
7. Krishnamurthy, K. N., Sridhara, S. N. & Ananda Kumar, C. S. Synthesis and optimization of hydnocarpus Wightiana and dairy waste scum as feed stock for biodiesel production by using response surface methodology. *Energy* https://doi.org/10.1016/j.energy.2018.04.068 (2018).
8. Özer, S., Gülcan, H. E., Çelebi, S. & Demir, U. Assessment of waste tyre pyrolysis oil and oxy-hydrogen gas usage in a diesel engine in terms of energy, exergy, environmental, and enviroeconomic perspectives. *Int. J. Hydrogen Energy*. **143**, 862–881. https://doi.org/10.1016/j.ijhydene.2024.11.107 (2025).
9. Özer, S., Tunçer, E., Demir, U. & Gülcan, H. E. Thermodynamic, thermoeconomic, and exergoeconomic analysis of a UAV two stroke engine fueled with gasoline-octanol and gasoline-hexanol blends. *Energy Convers. Manag.* **327**, 119545. https://doi.org/10.1016/j.enconman.2025.119545 (2025).
10. Krishnamurthy, K. N., Sridhara, S. N. & Ananda Kumar, C. S. Optimization and kinetic study of biodiesel production from hydnocarpus Wightiana oil and dairy waste scum using snail shell CaO nano catalyst. *Renew. Energy*. **146**, 280–296. https://doi.org/10.1016/j.renene.2019.06.161 (2020).
11. Osman, A. I. et al. Optimizing biodiesel production from waste with computational chemistry, machine learning and policy insights: a review. *Environ. Chem. Lett.* **22**, 1005–1071. https://doi.org/10.1007/s10311-024-01700-y (2024).
12. Samuelraj, D., Harish, V. & Jaichandar, S. The influence of thermal barrier coating on an LHR engine fueled by soybean biodiesel blended with various additive spectrums: performance, combustion, and emission analysis. *Heat. Transf.* **52**, 3839–3868. https://doi.org/10.1002/htj.22854 (2023).
13. Vijay Kumar, M. et al. Impact of a thermal barrier coating in low heat rejection environment area of a diesel engine. *Sustainability* **14**, 15801. https://doi.org/10.3390/su142315801 (2022).
14. Anjaneya, G. et al. Performance analysis and optimization of thermal barrier coated piston diesel engine fuelled with biodiesel using RSM. *Case Stud. Therm. Eng.* **57**, 104351. https://doi.org/10.1016/j.csite.2024.104351 (2024).
15. Manickam, S., Pachamuthu, S., Chavan, S. & Kim, S. C. The effect of thermal barrier coatings and neural networks on the stability, performance, and emission characteristics of Pongamia water emulsion biodiesel in compression ignition engines. *Case Stud. Therm. Eng.* **49**, 103079. https://doi.org/10.1016/j.csite.2023.103079 (2023).
16. Palani, V., Narayanan, S. G. & Kumar, A. R. P. Performance on multilayered nano-structured thermal barrier-coated compression ignition engine on green diesel. *J. Therm. Anal. Calorim.* https://doi.org/10.1007/s10973-025-14339-w (2025).
17. Sharma, S. K., Ojha, K. V., Pradhan, D., Kumari, P. & kumar, A. Analyses of temperature and thermal stresses of a Ceramic-Coated diesel engine valve, pp. 127–134. (2021). https://doi.org/10.1007/978-981-15-8704-7_15
18. Reddy, G. V. et al. Performance evaluation of low heat rejection diesel engine operated with biofuels under-selective catalytic reduction. *AIP Adv.* 14. https://doi.org/10.1063/5.0194458 (2024).
19. Bogdan, M. & Peter, I. A comprehensive Understanding of thermal barrier coatings (TBCs): applications, materials, coating design and failure mechanisms. *Met. (Basel)*. **14**, 575. https://doi.org/10.3390/met14050575 (2024).
20. Frank, R. M. & Heywood, J. B. The effect of piston temperature on hydrocarbon emissions from a spark-ignited direct-injection engine. *SAE Tech. Papers*. https://doi.org/10.4271/910558 (1991).
21. Jude, S. A. A., Jappes, J. T. W. & Adamkhan, M. Thermal barrier coatings for high-temperature application on Superalloy substrates - A review. *Mater. Today Proc.* **60**, 1670–1675. https://doi.org/10.1016/j.matpr.2021.12.223 (2022).
22. Bose, S. & High Temperature Coatings (2007). https://doi.org/10.1016/B978-0-7506-8252-7.X5000-8
23. Krupakaran, R. L. et al. The influence of thermal barrier coating (TBC) on diesel engine performance powered by using *Mimusops Elengi* Methyl ester with TiO_2 nanoadditive. *Int. J. Ambient Energy*. **44**, 2250–2261. https://doi.org/10.1080/01430750.2023.2231470 (2023).

24. Rohan, P. et al. Thermal and mechanical properties of cordierite, mullite and steatite produced by plasma spraying. *Ceram. Int.* **30**, 597–603. https://doi.org/10.1016/j.ceramint.2003.07.004 (2004).
25. Valiveti, S. R. K., Shaik, H. & Reddy, K. V. K. Analysis on impact of thermal barrier coating on piston head in CI engine using biodiesel. *Int. J. Ambient Energy*. **43**, 3377–3384. https://doi.org/10.1080/01430750.2020.1831592 (2022).
26. Hazar, H. Characterization and effect of using cotton Methyl ester as fuel in a LHR diesel engine. *Energy Convers. Manag.* **52**, 258–263. https://doi.org/10.1016/j.enconman.2010.06.066 (2011).
27. Aydin, H. Combined effects of thermal barrier coating and blending with diesel fuel on usability of vegetable oils in diesel engines. *Appl. Therm. Eng.* **51**, 623–629. https://doi.org/10.1016/j.applthermaleng.2012.10.030 (2013).
28. Jena, S. P., Acharya, S. K., Das, H. C., Patnaik, P. P. & Bajpai, S. Investigation of the effect of FeCl3 on combustion and emission of diesel engine with thermal barrier coating. *Sustainable Environ. Res.* **28**, 72–78. https://doi.org/10.1016/j.serj.2017.10.002 (2018).
29. Saravanan, P., Mala, D., Jayaseelan, V. & Nallapaneni Manoj Kumar. and. Experimental performance investigation of partially stabilized zirconia coated low heat rejection diesel engine with waste plastic oil as a fuel. Energy sources, part A: recovery, utilization, and environmental effects 45, 4 : 11046–11059. (2023). https://doi.org/10.1080/15567036.2019.1683647
30. Reddy, S. V. K. & Premkartikkumar, S. R. Radha Krishna gopidesi and nitin Uttamrao kautkar, A review on nano coatings for Ic engine applications. *Int. J. Mech. Eng. Technol.* **8** (9), 70–76 (2017). http://www.iaeme.com/IJMET/issues.asp?JType=IJMET&VType=8&IType=9
31. Senthil, R., Sivakumar, E., Silambarasan, R. & Pranesh, G. Performance and emission characteristics of using sea lemon biodiesel with thermal barrier coating in a direct-injection diesel engine. *Biofuels* **8**, 235–241. https://doi.org/10.1080/17597269.2016.1221299 (2017).
32. Hazar, H., Sevinc, H. & Sap, S. Performance and emission properties of preheated and blended fennel vegetable oil in a coated diesel engine. *Fuel* **254**, 115677. https://doi.org/10.1016/j.fuel.2019.115677 (2019).
33. Hazar, H. Cotton Methyl ester usage in a diesel engine equipped with insulated combustion chamber. *Appl. Energy*. **87**, 134–140. https://doi.org/10.1016/j.apenergy.2009.07.024 (2010).
34. Parlak, A., Yaşar, H., Haşimoğlu, C. & Kolip, A. The effects of injection timing on NO_x emissions of a low heat rejection indirect diesel injection engine. *Appl. Therm. Eng.* **25**, 3042–3052. https://doi.org/10.1016/j.applthermaleng.2005.03.012 (2005).
35. Rajendra Prasath, B., Tamilporai, P. & Shabir, M. F. Analysis of combustion, performance and emission characteristics of low heat rejection engine using biodiesel. *Int. J. Therm. Sci.* **49**, 2483–2490. https://doi.org/10.1016/j.ijthermalsci.2010.07.010 (2010).
36. Mohamed Musthafa, M., Sivapirakasam, S. P. & Udayakumar, M. Comparative studies on fly Ash coated low heat rejection diesel engine on performance and emission characteristics fueled by rice Bran and Pongamia Methyl ester and their blend with diesel. *Energy* **36**, 2343–2351. https://doi.org/10.1016/j.energy.2010.12.047 (2011).
37. Wu, G., Ge, J. C. & Nag Jung Choi A comprehensive review of the application characteristics of biodiesel blends in diesel engines. *Applied Sciences* 10, no. 22 : 8015. (2020). https://doi.org/10.3390/app10228015
38. Kumar, R. Combustion and emission characteristics of variable compression ignition engine fueled with Jatropha Curcas Ethyl ester blends at different compression ratio. *J. Renew. Energy*. **2014** (1), 872923. https://doi.org/10.1155/2014/872923 (2014).
39. Dhinesh, B., Maria Ambrose Raj, Y., Kalaiselvan, C. & KrishnaMoorthy, R. A numerical and experimental assessment of a coated diesel engine powered by high-performance nano biofuel. *Energy Convers. Manag.* **171**, 815–824. https://doi.org/10.1016/j.enconman.2018.06.039 (2018).
40. Gzate, Y. et al. Performance testing of moringa oleifera seed oil biodiesel with additives in diesel engine. *Heliyon* 10, no. 4 (2024). https://doi.org/10.1016/j.heliyon.2024.e26293
41. Elumalai, P. V., Annamalai, K. & Dhinesh, B. Effects of thermal barrier coating on the performance, combustion and emission of DI diesel engine powered by biofuel oil–water emulsion. *J. Therm. Anal. Calorim.* **137**, 593–605. https://doi.org/10.1007/s10973-018-7948-6 (2019).
42. Vedharaj, S. et al. Experimental and finite element analysis of a coated diesel engine fueled by cashew nut shell liquid biodiesel. *Exp. Therm. Fluid Sci.* **53**, 259–268. https://doi.org/10.1016/j.expthermflusci.2013.12.018 (2014).
43. Sivalingam, A., Venkatesan, E. P., Roberts, K. L. & Asif, M. Potential effect of lemon Peel oil with novel eco-friendly and biodegradable emulsion in un-modified diesel engine. *ACS Omega*. **8** (21), 18566–18581. https://doi.org/10.1021/acsomega.3c00325 (2023).
44. Viswanathan, K., Balasubramanian, D., Subramanian, T. & Varuvel, E. G. Investigating the combined effect of thermal barrier coating and antioxidants on pine oil in DI diesel engine. *Environ. Sci. Pollut. Res.* https://doi.org/10.1007/s11356-019-04649-6 (2019).
45. Karthickeyan, V., Thiyagarajan, S., Ashok, B., Edwin Geo, V. & Azad, A. K. Experimental investigation of pomegranate oil Methyl ester in ceramic coated engine at different operating condition in direct injection diesel engine with energy and exergy analysis. *Energy Convers. Manag.* **205**, 112334. https://doi.org/10.1016/j.enconman.2019.112334 (2020).
46. Sivasubramanian, H. Performance and emission characteristics of papaya seed oil methyl ester–n-butanol–diesel blends on a stationary direct-injection CI engine. *Biofuels* 9, no. 4 : 513–522. (2018). https://doi.org/10.1080/17597269.2017.1291878
47. Modi, A. J. & Patel, D. Experimental study on LHR diesel engine performance with blends of diesel and Neem biodiesel. *SAE Tech. Papers*. https://doi.org/10.4271/2015-26-0188 (2015).
48. Aydin, S., Sayin, C. & Aydin, H. Investigation of the usability of biodiesel obtained from residual frying oil in a diesel engine with thermal barrier coating. *Appl. Therm. Eng.* **80**, 212–219. https://doi.org/10.1016/j.applthermaleng.2015.01.061 (2015).
49. Karthickeyan, V. Effect of combustion chamber bowl geometry modification on engine performance, combustion and emission characteristics of biodiesel fuelled diesel engine with its energy and exergy analysis. *Energy* **176**, 830–852. https://doi.org/10.1016/j.energy.2019.04.012 (2019).
50. Venkatesan, E. P. et al. Experimental studies on Thermal-Barrier-Coated engine fuelled by a blend of Eucalyptus oil and DEE. *ACS Omega*. **7**, 46391–46401. https://doi.org/10.1021/acsomega.2c05089 (2022).
51. Hejwowski, T. & Weroński, A. The effect of thermal barrier coatings on diesel engine performance. *Vacuum* **65**, 427–432. https://doi.org/10.1016/S0042-207X(01)00452-3 (2002).
52. Krishnamoorthi, M. & Malayalamurthi, R. Experimental investigation on performance, emission behavior and exergy analysis of a variable compression ratio engine fueled with diesel - aegle Marmelos oil - diethyl ether blends. *Energy* **128**, 312–328. https://doi.org/10.1016/j.energy.2017.04.038 (2017).
53. Ağbulut, Ü., Sarıdemir, S. & Albayrak, S. Experimental investigation of combustion, performance and emission characteristics of a diesel engine fuelled with diesel–biodiesel–alcohol blends. *J. Brazilian Soc. Mech. Sci. Eng.* 2019;41. https://doi.org/10.1007/s40430-019-1891-8
54. Yesilyurt, M. K. A detailed investigation on the performance, combustion, and exhaust emission characteristics of a diesel engine running on the blend of diesel fuel, biodiesel and 1-heptanol (C7 alcohol) as a next-generation higher alcohol. *Fuel* **275**, 117893. https://doi.org/10.1016/j.fuel.2020.117893 (2020).
55. Krishnamoorthi, T., Sudalaimuthu, G., Dillikannan, D. & Jayabal, R. Influence of thermal barrier coating on performance and emission characteristics of a compression ignition engine fueled with Delonix regia seed biodiesel. *J. Clean. Prod.* **420**, 138413. https://doi.org/10.1016/j.jclepro.2023.138413 (2023).
56. Ozsezen, A. N. & Canakci, M. Determination of performance and combustion characteristics of a diesel engine fueled with Canola and waste palm oil Methyl esters. *Energy Convers. Manag.* **52**, 108–116. https://doi.org/10.1016/j.enconman.2010.06.049 (2011).
57. Fayad, M. A. et al. Reducing soot nanoparticles and NO_x emissions in CRDI diesel engine by incorporating TiO2 Nano-Additives into biodiesel blends and using high rate of EGR. *Energies (Basel)*. **16**, 3921. https://doi.org/10.3390/en16093921 (2023).

58. Krishnamoorthi, T., Sampath, S., Saravanamuthu, M., Vengadesan, E. & Dillikannan, D. Combined influence of thermal barrier coating and nanoparticle on performance and emissions of DI diesel engine fueled with neat palm oil biodiesel: an experimental, statistical and energy and exergy analysis. *Process Saf. Environ. Prot.* **186**, 274–288. https://doi.org/10.1016/j.psep.2024.03.108 (2024).
59. Soudagar, M. E. M., Afzal, A. & Kareemullah, M. Waste coconut oil Methyl ester with and without additives as an alternative fuel in diesel engine at two different injection pressures. *Energy Sour. Part A Recover. Utilization Environ. Eff.* **46**, 8751–8769. https://doi.org/10.1080/15567036.2020.1769775 (2024).
60. Muralidharan, K. & Vasudevan, D. Performance, emission and combustion characteristics of a variable compression ratio engine using Methyl esters of waste cooking oil and diesel blends. *Appl. Energy*. **88**, 3959–3968. https://doi.org/10.1016/j.apenergy.2011.04.014 (2011).
61. Fayad, M. A. et al. Incorporating of TiO2 with oxygenated fuel and post-injection strategy in CRDI diesel engine equipped with EGR: A step towards lower NO_x, PM and enhance soot oxidation reactivity. *Case Stud. Therm. Eng.* **53**, 103894. https://doi.org/10.1016/j.csite.2023.103894 (2024).
62. Shrirao, P. N. & Pawar, A. N. Evaluation of performance and emission characteristics of turbocharged diesel engine with mullite as thermal barrier coating. *Int. J. Eng. Technol.* **3**, 256–262 (2011).
63. Yao, M., Ma, T., Wang, H., Zheng, Z. & Zhang, Y. Haifeng Liu, and A theoretical study on the effects of thermal barrier coating on diesel engine combustion and emission characteristics. Energy 162 : 744–752. (2018). https://doi.org/10.1016/j.energy.2018.08.009
64. Yatish, K. V., Lalithamba, H. S., Suresh, R. & Harsha Hebbar, H. R. Optimization of bauhinia variegata biodiesel production and its performance, combustion and emission study on diesel engine. *Renew. Energy*. **122**, 561–575. https://doi.org/10.1016/j.renene.2018.01.124 (2018).
65. Özener, O., Yüksek, L., Ergenç, A. T. & Özkan, M. Effects of soybean biodiesel on a DI diesel engine performance, emission and combustion characteristics. *Fuel* **115**, 875–883. https://doi.org/10.1016/j.fuel.2012.10.081 (2014).
66. Veeraraghavan, S., De Poures, M. V., Madhu, S. & Palani, K. Enhancing diesel engine performance with silica coated pistons and Cassia fistula biodiesel blends: A pathway to cleaner and efficient energy, (2024). https://doi.org/10.4271/2024-01-5222
67. Ramesh, A. et al. Influence of hexanol as additive with Calophyllum Inophyllum biodiesel for CI engine applications. *Fuel* **249**, 472–485. https://doi.org/10.1016/j.fuel.2019.03.072 (2019).
68. Yesilyurt, M. K., Aydin, M., Yilbasi, Z. & Arslan, M. Investigation on the structural effects of the addition of alcohols having various chain lengths into the vegetable oil-biodiesel-diesel fuel blends: an attempt for improving the performance, combustion, and exhaust emission characteristics of a compressi. *Fuel* **269**, 117455. https://doi.org/10.1016/j.fuel.2020.117455 (2020).
69. Reddy Rm, S. et al. Experimental investigation on thermal Barrier-Coated diesel engine using Antioxidant-Doped orange Peel oil biodiesel. *Surf. Rev. Lett.* https://doi.org/10.1142/S0218625X24501270 (2024).
70. Alagumalai, A. Combustion characteristics of Lemongrass (Cymbopogon flexuosus) oil in a partial premixed charge compression ignition engine. *Alexandria Eng. J.* **54**, 405–413. https://doi.org/10.1016/j.aej.2015.03.021 (2015).
71. Ağbulut, Ü., Sarıdemir, S. & Albayrak, S. Experimental investigation of combustion, performance and emission characteristics of a diesel engine fuelled with diesel–biodiesel–alcohol blends. *J. Brazilian Soc. Mech. Sci. Eng.* **41**, 389. https://doi.org/10.1007/s40430-019-1891-8 (2019).
72. Can, Ö. Combustion characteristics, performance and exhaust emissions of a diesel engine fueled with a waste cooking oil biodiesel mixture. *Energy Convers. Manag.* **87**, 676–686. https://doi.org/10.1016/j.enconman.2014.07.066 (2014).
73. Öztürk, E. Performance, emissions, combustion and injection characteristics of a diesel engine fuelled with Canola oil-hazelnut soapstock biodiesel mixture. *Fuel Process. Technol.* **129**, 183–191. https://doi.org/10.1016/j.fuproc.2014.09.016 (2015).
74. Nagaraja, S., Soorya Prakash, K., Sudhakaran, R. & Sathish Kumar, M. Investigation on the emission quality, performance and combustion characteristics of the compression ignition engine fueled with environmental friendly corn oil Methyl ester – Diesel blends. *Ecotoxicol. Environ. Saf.* **134**, 455–461. https://doi.org/10.1016/j.ecoenv.2016.01.023 (2016).
75. Santhoshkumar, A., Thangarasu, V. & Anand, R. *Performance, Combustion, and Emission Characteristics of DI Diesel Engine Using Mahua Biodiesel* (Elsevier Ltd, 2019). https://doi.org/10.1016/B978-0-08-102791-2.00012-X
76. Gülcan, H. E., Erol, D., Çelik, M. & Bayındırlı, C. Assessment of trade-off, exergetic performance, and greenhouse gas impact-cost analysis of a diesel engine running with different proportions of TiO_2, Ag_2O, and CeO_2 nanoadditives. *Energy* **313**, 133786. https://doi.org/10.1016/j.energy.2024.133786 (2024).
77. Shrivastava, P., Salam, S., Verma, T. N. & Samuel, O. D. Experimental and empirical analysis of an IC engine operating with ternary blends of diesel, Karanja and roselle biodiesel. *Fuel* **262**, 116608. https://doi.org/10.1016/j.fuel.2019.116608 (2020).
78. Sivaramakrishnan, K. Investigation on performance and emission characteristics of a variable compression multi fuel engine fuelled with Karanja biodiesel–diesel blend. *Egypt. J. Petroleum.* **27**, 177–186. https://doi.org/10.1016/j.ejpe.2017.03.001 (2018).
79. Hirkude, J. & Padalkar, A. S. Experimental investigation of the effect of compression ratio on performance and emissions of CI engine operated with waste fried oil methyl ester blend. Fuel Processing Technology. ;128:367–75. (2014). https://doi.org/10.1016/j.fuproc.2014.07.026
80. Ramasamy, N., Kalam, M. A., Varman, M. & Teoh, Y. H. Effect of thermal barrier coating on the performance and emissions of diesel engine operated with conventional diesel and palm oil biodiesel. *Coatings* **11**, 692. https://doi.org/10.3390/coatings11060692 (2021).
81. Appavu, P., Ramanan, M. V. & Venu, H. Quaternary blends of diesel/biodiesel/vegetable oil/pentanol as a potential alternative feedstock for existing unmodified diesel engine: performance, combustion and emission characteristics. Energy 2019;186. https://doi.org/10.1016/j.energy.2019.115856
82. Venu, H., Raju, V. D., Subramani, L. & Appavu, P. *Experimental Assessment on the Regulated and Unregulated Emissions of DI Diesel Engine Fuelled with Chlorella Emersonii Methyl Ester (CEME)*vol. 151 (Elsevier B.V., 2020). https://doi.org/10.1016/j.renene.2019.11.010
83. Yaliwal, V. S. & Banapurmath, N. R. Combustion and emission characteristics of a compression ignition engine operated on dual fuel mode using renewable and sustainable fuel combinations. *SN Appl. Sci.* **3**, 24. https://doi.org/10.1007/s42452-020-03987-2 (2021).
84. Wang, Z. and Xiaoyi Yang. NOx Formation Mechanism and Emission Prediction in Turbulent Combustion: A Review. *Applied Sciences (* 14, no. 14 (2024). (2076).
85. Viswanathan, K. & Wang, S. Experimental investigation on the application of preheated fish oil Ethyl ester as a fuel in diesel engine. *Fuel* **285**, 119244. https://doi.org/10.1016/j.fuel.2020.119244 (2021).
86. Viswanathan, K., Ashok, B. & Pugazhendhi, A. Comprehensive study of engine characteristics of novel biodiesel from curry leaf (Murraya koenigii) oil in ceramic layered diesel engine. *Fuel* **280**, 118586. https://doi.org/10.1016/j.fuel.2020.118586 (2020).
87. Praveena, V. & Leenus Jesu Martin, M. A review on various after treatment techniques to reduce nox emissions in a CI engine. *J. Energy Inst.* **91** (5), 704–720. https://doi.org/10.1016/j.joei.2017.05.010 (2018).
88. Can, Ö., Öztürk, E. & Yücesu, H. S. Combustion and exhaust emissions of Canola biodiesel blends in a single cylinder DI diesel engine. *Renew. Energy* **109**, 73–82. https://doi.org/10.1016/j.renene.2017.03.017. (2017).

Acknowledgements

"The authors extend their appreciation to the Deanship of Research and Graduate Studies at King Khalid University for funding this work through Large Research Project under grant number RGP2/491/46. The authors

would also like to express their sincere gratitude to DoS in Mechanical Engineering, Centre for Post Graduate studies, Visvesvaraya Technological University, Mysuru, Karnataka, India for providing VCR Diesel Engine Experimental Setup to conduct various performance test research facility that is very much necessary to carry out the present research study.

Author contributions

Conceptualization, K.K.N, A.D B.N; Writing—Review and Editing, V.B.J, S.C.P; Methodology, A.K; Formal analysis, S.K, Investigation and Supervision, S.I A.R, Y.D.J.

Funding

The authors extend their appreciation to the Deanship of Research and Graduate Studies at King Khalid University for funding this work through Large Research Project under grant number RGP2/491/46.

Declarations

Competing interests

The authors declare no competing interests.

Conflict interests

The authors declare that they have no conflict of interest.""The authors declare that they have no conflict of interest.

Additional information

Supplementary Information The online version contains supplementary material available at https://doi.org/10.1038/s41598-025-14591-y.

Correspondence and requests for materials should be addressed to K.K.N. or Y.D.J.

Reprints and permissions information is available at www.nature.com/reprints.

Publisher's note Springer Nature remains neutral with regard to jurisdictional claims in published maps and institutional affiliations.